NASA TECHNICAL NOTE

NASA TN D-6154

AXISYMMETRIC EXPANSION OF A PLASMA IN A MAGNETIC NOZZLE INCLUDING THERMAL CONDUCTION

by Eddie L. Walker and George R. Seikel

Lewis Research Center
Cleveland, Ohio 44135

NATIONAL AERONAUTICS AND SPACE ADMINISTRATION • WASHINGTON, D. C. • FEBRUARY 1971

1. Report No.	2. Government Accession No.	3. Recipient's
NASA TN D-6154		

4. Title and Subtitle
AXISYMMETRIC EXPANSION OF A PLASMA IN A MAGNETIC NOZZLE INCLUDING THERMAL CONDUCTION

5. Report Date
February 1971

6. Performing Organization Code

7. Author(s)
Eddie L. Walker and George R. Seikel

8. Performing Organization Report No.
E-5888

10. Work Unit No.
120-26

9. Performing Organization Name and Address
Lewis Research Center
National Aeronautics and Space Administration
Cleveland, Ohio 44135

11. Contract or Grant No.

13. Type of Report and Period Covered
Technical Note

12. Sponsoring Agency Name and Address
National Aeronautics and Space Administration
Washington, D.C. 20546

14. Sponsoring Agency Code

15. Supplementary Notes

16. Abstract

The axisymmetric expansion of a fully ionized, hot-electron cold-ion plasma in a magnetic nozzle is analyzed with thermal conduction included. Computed is the on-axis ratio of the directed ion exhaust energy to the maximum (upstream) electron thermal energy as a function of two parameters: (1) the on-axis sonic point location, and (2) a dimensionless magnetic field which involves the ratio of the maximum value of the applied magnetic field to an effective electron Hall parameter. The results differ sharply from that of an adiabatic expansion, with the energy ratio attaining values more than an order of magnitude greater than the adiabatic value. Limitations of the analysis are discussed along with an application to low power MPD arc thrusters.

17. Key Words (Suggested by Author(s))	18. Distribution Statement
Plasma expansion; Fully ionized; Magnetic nozzle; Thermal conduction; Magnetoplasmadynamic arc; Electron temperature; Ion exhaust energy; Energy ratio; Sonic point; Hall parameter; Asymptotic solution	Unclassified - unlimited

19. Security Classif. (of this report)	20. Security Classif. (of this page)	21. No. of Pages	22. Price*
Unclassified	Unclassified	62	$3.00

*For sale by the National Technical Information Service, Springfield, Virginia 22151

CONTENTS

	Page
SUMMARY	1
INTRODUCTION	2
THEORETICAL ANALYSIS	3
Assumptions	3
Kinetic Equations	4
Continuity equations	4
Momentum equations	5
Electron energy equation	8
Transport Coefficients	8
Momentum collision integral coefficients	8
Energy collision integral coefficient	9
Electron heat flow coefficients	10
The effective electron Hall parameter	11
Final Equations	12
NUMERICAL SOLUTIONS	16
Asymptotic Analytic Solutions	16
Numerical Procedure	19
Starting calculations	19
Numerical integration	23
RESULTS AND DISCUSSION	24
Singularity at Maximum Electron Temperature	24
Axial Variation of Plasma Quantities	25
Spatial Dependence of U and τ on β	26
Ratio of Final Ion to Initial Electron Energy	26
Limitations of Analysis	27
Significance of Results	29
CONCLUDING REMARKS	29
APPENDIXES	
A - SYMBOLS	31
B - THE APPLIED MAGNETIC FIELD	33
C - MAGNITUDE OF FIELD QUANTITIES	35

D - THE ELECTRON HEAT FLOW. 39
E - THE ASYMPTOTIC SERIES 43
F - THE SINGULARITY POINT 48
G - THE ADIABATIC SOLUTION. 50

REFERENCES 53

AXISYMMETRIC EXPANSION OF A PLASMA IN A MAGNETIC NOZZLE INCLUDING THERMAL CONDUCTION

by Eddie L. Walker and George R. Seikel

Lewis Research Center

SUMMARY

The axisymmetric expansion of a hot-electron, cold-ion plasma in the magnetic nozzle produced by a pair of Helmholtz coils is calculated with thermal conduction included. The plasma is assumed fully ionized (in the sense that neutrals have no significant effect on the expansion) and the electron Hall parameter is assumed to have an effective constant value. The analysis is based on the reduction of the partial differential kinetic equations to ordinary differential equations which are valid near the axis of symmetry. The resulting nonlinear coupled equations were solved numerically by starting far downstream with the leading terms of an analytic asymptotic solution and working upstream. The numerical results depend on two parameters: (1) the location of the on-axis sonic point, and (2) a dimensionless magnetic field β, which involves the ratio of the maximum value of the applied magnetic field to the effective electron Hall parameter.

The analysis predicts the spatial variation along the axis of symmetry of the ion flow velocity, electron temperature, plasma potential, and electron number density. Also presented is the dependence on β of the spatial variation of the on-axis ion flow velocity and electron temperature. The analysis appears to be consistent with available experimental data.

The final results give the on-axis ratio of the directed ion exhaust energy to the maximum (upstream) electron thermal energy as a function of the sonic point location and the dimensionless magnetic field β. The effect of including thermal conduction is striking; the energy ratio attains values more than an order of magnitude greater than that for an adiabatic expansion.

The analysis is valid for a finite range of the parameter β. The largest value of β is limited by the stated assumption that the ion temperature is negligible, while the smallest value is limited by the implicit assumption of small electron cyclotron radii.

INTRODUCTION

Those performing research on magnetoplasmadynamic (MPD) arc thrusters have for a number of years been investigating the steady-state acceleration of plasma in a magnetic nozzle. In an early paper (ref. 1) the following model of this process was deduced for low-density dc discharge thrusters (i.e., long ion mean free path):

> The electric power of the discharge is primarily added to the random energy of the plasma electrons. The energetic electrons ionize the propellant, and, as the plasma's electron gas expands out of the device, its random electron energy is converted to directed energy. Since there can be no divergence of current, however, the electrons drag the ions along. Physically this is accomplished by an axial electric field that the plasma itself builds. This field retards the electrons' expansion, accelerates the ions, and causes an azimuthal electron current to flow that provides the electromagnetic reaction force on the accelerator. The energy added to the ions is at the expense of the random electron energy. The expansion process is controlled by the magnetic nozzle action of the spatially varying magnetic field.

The existence of this plasma generated axial electric field was supported by the experiments of Domitz (ref. 2) and the research of Meyerand et al. (ref. 3).

In a later paper (ref. 4) it was shown that on the axis of symmetry this axial electric field was given by the gradient of the electron pressure divided by the electron charge density. Subsequent experiments by Bowditch (ref. 5) show that this relation for the axial electric field was applicable in the exhaust field of a fully ionized, low-power thruster. Hence, his results experimentally substantiated the proposed acceleration model.

A detailed examination of the data of reference 5 shows, in addition, that the plasma expansion process is not adiabatic. The exhaust ion energy measured is much higher than one would obtain in an adiabatic expansion. And the electron temperature does not spatially decrease as rapidly as one would expect in an adiabatic expansion.

For the electron temperature range of 5 to 10 electron volts measured by Bowditch, a plasma is a good thermal conductor. Thus, thermal conduction can be important.

The object of this study is to analyze the expansion of a plasma in a magnetic nozzle including thermal conduction. Specifically, the expansion of a fully ionized plasma containing hot electrons and cold ions is examined in the magnetic nozzle produced by a Helmholtz set of coils. (The phrase "fully ionized" simply means here that any neutrals which may be present play no appreciable role in the expansion.) The analysis is restricted to the vicinity of the axis of symmetry. The set of equations to be solved

includes the electron and ion continuity and momentum equations, Maxwell's equations and an electron energy equation. As indicated in reference 6, the solutions can be used in an energy balance which leads to setting upper bounds on the potential performance of applicable MPD arc thrusters. Finally, the limits on applications of the analysis are discussed along with the results.

THEORETICAL ANALYSIS

In this section Maxwell's equations, the electron and ion continuity and momentum equations, and the electron energy equation are combined to obtain two coupled nonlinear ordinary differential equations for the electron temperature and ion flow velocity. The equations are valid for points near the axis of symmetry, with the effective electron Hall parameter and the magnetic field appearing as parameters.

Assumptions

The coordinate system for the plasma expansion is shown in figure 1. In order to reduce the usual kinetic equations to ordinary differential equations it is assumed that each variable of interest can be expanded in a power series in the radial coordinate r near the axis of symmetry. Then for instance, the electron temperature T_e is given by

$$T_e = T_e(r, z) = T_e^{(0)}(z) + rT_e^{(1)}(z) + r^2T_e^{(2)}(z) + \cdots \tag{1}$$

so that the electron temperature on the axis is simply

$$T_e(r = 0, z) = T_e^{(0)}(z) \tag{2}$$

By expanding each variable in this manner, substituting the series into the partial differential kinetic equations, and comparing coefficients of like powers of r, ordinary differential equations are obtained for the electron temperature and ion flow velocity on the axis.

In deriving the final equations, the following additional assumptions are made (symbols are defined in appendix A and all equations and quantities are in S.I. units):

(1) Steady state exists, $\partial/\partial t \equiv 0$.

(2) Neutrals have no significant effect on the expansion (equivalent to assuming a fully ionized plasma).

(3) The species pressures are scalar; that is, viscous effects are negligible.

(4) $T_i \ll T_e$.

(5) Quasi-charge neutrality exists on the axis, $N_e^{(0)} = N_i^{(0)}$.

(6) There is no axial current density on the axis, $J_z^{(0)} = 0$.

(7) The on-axis induced magnetic field is negligible compared to the applied field. (Appendix B contains a discussion of the applied magnetic field.)

(8) The electron inertia term in the electron momentum equation is neglected.

(9) Inelastic collisions are negligible.

Kinetic Equations

The conduction current density is given by

$$\vec{J} = q(N_i\vec{u}_i - N_e\vec{u}_e) \tag{3}$$

From the assumptions

$$J_z^{(0)} = 0 \tag{4}$$

and

$$N_e^{(0)} = N_i^{(0)} \tag{5}$$

it then follows that

$$u_{e,z}^{(0)} = u_{i,z}^{(0)} \tag{6}$$

Continuity equations. - The electron continuity equation is

$$\nabla \cdot (N_e\vec{u}_e) = 0 \tag{7}$$

or

$$\frac{1}{r}\frac{\partial}{\partial r}(rN_e u_{e,r}) + \frac{\partial}{\partial z}(N_e u_{e,z}) = 0$$

from which,

$$u_{e,r}^{(0)} = 0 \tag{8a}$$

$$u_{e,r}^{(1)} = -\frac{1}{2N_e^{(0)}} \frac{d}{dz} \left[N_e^{(0)} u_{e,z}^{(0)} \right] \tag{8b}$$

where it has been assumed that $N_e^{(0)} \neq 0$. Completely analogous results are found for the ion flow velocity coefficients:

$$u_{i,r}^{(0)} = 0 \tag{8c}$$

$$u_{i,r}^{(1)} = -\frac{1}{2N_i^{(0)}} \frac{d}{dz} \left[N_i^{(0)} u_{i,z}^{(0)} \right] \tag{8d}$$

Momentum equations. - The electron and ion momentum equations are, respectively,

$$\nabla P_e + qN_e \left(\vec{E} + \vec{u}_e \times \vec{B} \right) = \vec{I}_e \tag{9}$$

$$N_i m_i \vec{u}_i \cdot \nabla \vec{u}_i - qN_i \left(\vec{E} + \vec{u}_i \times \vec{B} \right) = -\vec{I}_e \tag{10}$$

where the ion scalar pressure and the gravitational acceleration have been neglected. Since $E_\theta = 0$ (see appendix C, eq. (C15)), the θ-component of the sum of equations (9) and (10) is

$$N_i m_i \left(\vec{u}_i \cdot \nabla \vec{u}_i \right)_\theta - (J_z B_r - J_r B_z) = 0 \tag{11}$$

Since B_r is of order r and J_r is of order r^2 (see eqs. (C10) and (C24), respectively), it follows that, to first order in r,

$$\left(\vec{u}_i \cdot \nabla \vec{u}_i \right)_\theta = 0 \tag{12}$$

Now from equation (12) it is possible to show that $u_{i,\theta}$ is of order r^2. First, using the assumption $\partial/\partial\theta = 0$ yields

$$\left(\vec{u}_i \cdot \nabla\vec{u}_i\right)_\theta = u_{i,r}\frac{\partial u_{i,\theta}}{\partial r} + \frac{u_{i,\theta}u_{i,r}}{r} + u_{i,z}\frac{\partial u_{i,\theta}}{\partial z} \tag{13}$$

Then, the substitution of the r-expansions into equation (13) and the use of equation (12) give

$$2u^{(1)}_{i,r}u^{(1)}_{i,\theta} + u^{(0)}_{i,z}\frac{du^{(1)}_{i,\theta}}{dz} = 0 \tag{14}$$

where the fact that $u^{(0)}_{i,\theta} = 0$ has been used. (The azimuthal component of velocity must vanish on the axis.) Substituting the result (8d) into equation (14) yields

$$\frac{d \ln u^{(1)}_{i,\theta}}{dz} - \frac{d \ln \left[N^{(0)}_i u^{(0)}_{i,z}\right]}{dz} = 0 \tag{15}$$

The solution of equation (15) is simply

$$u^{(1)}_{i,\theta} = KN^{(0)}_i u^{(0)}_{i,z} \tag{16}$$

where K is a constant. The ions are assumed to be monoenergetic, being created at some plane $z = z^*$ with no azimuthal velocity:

$$u_{i,\theta}(z = z^*) = 0 \tag{17}$$

It then follows from the expansion

$$u_{i,\theta} = ru^{(1)}_{i,\theta}(z) + r^2u^{(2)}_{i,\theta}(z) + \cdots$$

that

$$u^{(1)}_{i,\theta}(z^*) = 0$$

and hence the constant K in equation (16) must vanish, assuming that

$$N^{(0)}_i u^{(0)}_{i,z}\Big|_{z=z^*} \neq 0$$

Finally,

$$u_{i,\theta}^{(0)}(z) = u_{i,\theta}^{(1)}(z) \equiv 0 \tag{18}$$

The r-component of the ion momentum equation (10) is

$$N_i m_i \left(u_{i,r} \frac{\partial u_{i,r}}{\partial r} - \frac{u_{i,\theta}^2}{r} + u_{i,z} \frac{\partial u_{i,r}}{\partial z} \right) - qN_i(E_r + u_{i,\theta} B_z - u_{i,z} B_\theta) = - I_{e,r} \tag{19}$$

which to first order in r becomes

$$N_i^{(0)} m_i \left\{ \left[u_{i,r}^{(1)} \right]^2 + u_{i,z}^{(0)} \frac{du_{i,r}^{(1)}}{dz} \right\} - qN_i^{(0)} E_r^{(1)} = - I_{e,r}^{(1)} \tag{20}$$

where equations (8c), (18), and the results of appendix C, equations (C5) and (C20), have been used. Substituting the results (8d) and (C21) into equation (20) gives

$$\frac{m_i N_i^{(0)}}{2} \left(\frac{1}{2\left[N_i^{(0)}\right]^2} \left\{ \frac{d}{dz} \left[N_i^{(0)} u_{i,z}^{(0)} \right] \right\}^2 - u_{i,z}^{(0)} \frac{d}{dz} \left\{ \frac{1}{N_i^{(0)}} \frac{d}{dz} \left[N_i^{(0)} u_{i,z}^{(0)} \right] \right\} \right)$$

$$+ \frac{qN_i^{(0)}}{2} \frac{dE_z^{(0)}}{dz} = - I_{e,r}^{(1)} \tag{21}$$

The z-component of the electron momentum equation (9) is

$$\frac{\partial P_e}{\partial z} + qN_e(E_z + u_{e,r} B_\theta - u_{e,\theta} B_r) = I_{e,z} \tag{22}$$

which, to zero order in r, is

$$\frac{dP_e^{(0)}}{dz} + qN_e^{(0)} E_z^{(0)} = I_{e,z}^{(0)} \tag{23}$$

The z-component of the sum of equations (9) and (10) is

$$m_i N_i \left(u_{i,r} \frac{\partial u_{i,z}}{\partial r} + u_{i,z} \frac{\partial u_{i,z}}{\partial z} \right) + \frac{\partial P_e}{\partial z} + q(N_e - N_i)E_z - (J_r B_\theta - J_\theta B_r) = 0 \qquad (24)$$

which to zero order in r becomes

$$m_i N_i^{(0)} u_{i,z}^{(0)} \frac{du_{i,z}^{(0)}}{dz} + \frac{dP_e^{(0)}}{dz} = 0 \qquad (25)$$

Electron energy equation. - The final kinetic equation to be considered is the electron energy equation

$$\frac{3}{2} \vec{u}_e \cdot \nabla P_e + \frac{5}{2} P_e \nabla \cdot \vec{u}_e + \nabla \cdot \vec{Q}_e = I_E \qquad (26)$$

where $\vec{Q}_e$ and I_E are, respectively, the electron heat flow and the electron energy collision integral. To zero order in r, equation (26) becomes

$$\frac{3}{2} u_{e,z}^{(0)} \frac{dP_e^{(0)}}{dz} + \frac{5}{2} P_e^{(0)} \left[\frac{du_{e,z}^{(0)}}{dz} + 2u_{e,r}^{(1)} \right] + 2Q_{e,r}^{(1)} + \frac{dQ_{e,z}^{(0)}}{dz} = I_E^{(0)} \qquad (27)$$

(As is shown in appendix D, the radial electron heat flow vanishes on the axis, so that $Q_{e,r}^{(0)} = 0$.) Substituting equation (8b) into (27) gives

$$\frac{3}{2} u_{e,z}^{(0)} \frac{dP_e^{(0)}}{dz} - \frac{5}{2} P_e^{(0)} u_{e,z}^{(0)} \frac{d \ln N_e^{(0)}}{dz} + 2Q_{e,r}^{(1)} + \frac{dQ_{e,z}^{(0)}}{dz} = I_E^{(0)}$$

In order to close the set of equations (5), (6), (21), (23), (25), and (28), it remains to determine the collision integral coefficients $I_{e,r}^{(1)}$, $I_{e,z}^{(0)}$, $I_E^{(0)}$ and the electron heat flow coefficients $Q_{e,z}^{(0)}$, $Q_{e,r}^{(1)}$.

Transport Coefficients

Momentum collision integral coefficients. - The diffusion Mach number, which is defined as

$$\epsilon = \frac{\left|\vec{u}_i - \vec{u}_e\right|}{\left[2k\left(\frac{T_i}{m_i} + \frac{T_e}{m_e}\right)\right]^{1/2}}$$

is zero on the axis of symmetry by virtue of equations (6), (8a), (8c), and the fact that the azimuthal components of the electron and ion flow velocities must vanish at $r = 0$. From this fact it is reasonable to assume that ϵ is small in the vicinity of the axis of symmetry. Then, based on the well-known Grad-thirteen moment approximation for the electron and ion distribution functions, the electron momentum collision integral is, to first order in ϵ and in the dimensionless heat flows $Q_e \Big/ P_e\sqrt{2k\,T_e/m_e}$ and $Q_i \Big/ P_i\sqrt{2k\,T_i/m_i}$,

$$\vec{I}_e = m_e N_e \nu_{ei}\left[\left(\vec{u}_i - \vec{u}_e\right) + \frac{\gamma\vec{Q}_e}{P_e}\right] \tag{29}$$

Here ν_{ei} is the effective collision frequency for transfer of momentum between electrons and ions, and γ is a dimensionless number of order unity involving the interparticle force law (for the usual Coulomb force, $\gamma = 0.6$). The derivation of equation (29) is a straightforward but tedious process; the details can be found in reference 7. The result depends in part on the assumption that $Q_i/m_i \ll Q_e/m_e$.

Substituting the results (eqs. (5), (6), and (8a) to (8d)) into equation (29) yields

$$I_{e,z}^{(0)} = \frac{\gamma m_e N_e^{(0)} \nu_{ei}^{(0)} Q_{e,z}^{(0)}}{P_e^{(0)}} \tag{30a}$$

$$I_{e,r}^{(0)} = 0 \tag{30b}$$

$$I_{e,r}^{(1)} = \frac{\gamma m_e N_e^{(0)} \nu_{ei}^{(0)} Q_{e,r}^{(1)}}{P_e^{(0)}} \tag{30c}$$

The result (30b) depends on the fact that $Q_{e,r}^{(0)} = 0$, as shown in appendix D.

Energy collision integral coefficient. - From reference 7, the electron energy collision integral at $r = 0$ is

$$I_E^{(0)} = 3\left(\frac{m_e}{m_i}\right) N_e^{(0)} \nu_{ei}^{(0)} k \left(T_i^{(0)} - T_e^{(0)}\right), \tag{31a}$$

where note has been made of the fact that the diffusion Mach number ϵ is zero on the axis of symmetry. Then, since $T_i^{(0)} \ll T_e^{(0)}$, expression (31a) becomes

$$I_E^{(0)} = -3\left(\frac{m_e}{m_i}\right) \nu_{ei}^{(0)} P_e^{(0)} \tag{31b}$$

Electron heat flow coefficients. - Based on the same assumptions made in the discussion of the momentum collision integral coefficients, the z-component of the electron heat flow to order zero in r is

$$Q_{e,z}^{(0)} = -\frac{5}{2} \frac{P_e^{(0)}}{\mathcal{E} m_e \nu_{ei}^{(0)}} \frac{dkT_e^{(0)}}{dz} \tag{32a}$$

where $\mathcal{E}$ is a dimensionless number involving the interparticle force law (for the Coulomb force, $\mathcal{E} \cong 1.86$). The r-component coefficients of $\vec{Q}_e$ are

$$Q_{e,r}^{(0)} = 0 \tag{32b}$$

$$Q_{e,r}^{(1)} = \frac{\left[\omega_e^{(0)} \tau_e^{(0)}\right]}{2} \left\{\mathcal{E}^2 + \left[\omega_e^{(0)} \tau_e^{(0)}\right]^2\right\}^{-1} \left\{-\frac{10\mathcal{E} P_e^{(0)}}{qB^{(0)}} kT_e^{(2)}\right.$$

$$\left. - 5\gamma P_e^{(0)} u_{e,\theta}^{(1)} - \frac{5\left[\omega_e^{(0)} \tau_e^{(0)}\right]^2}{\mathcal{E} q} \frac{B_r^{(1)}}{\left[B^{(0)}\right]^2} P_e^{(0)} \frac{dkT_e^{(0)}}{dz}\right\} \tag{32c}$$

The results (32a) to (32c) are derived in appendix D. Implicit in their derivation is the use of the "transport approximation" wherein the mean time between collisions for the electrons and the electron mean free path are assumed to be small compared to, respectively, the characteristic time and distance intervals for significant changes in the non-Maxwellian part of the electron distribution function. In expression (32c) the electron cyclotron frequency is given by

$$\omega_e = \frac{qB}{m_e} \tag{33}$$

and

$$\tau_e = \frac{1}{\nu_{ei}} \tag{34}$$

It is noted that equation (32c) contains two new unknowns, $T_e^{(2)}$ and $u_{e,\theta}^{(1)}$. Hence, in order to close the set of equations (5), (6), (21), (23), (25), and (28), expression (32c) will not be used. Instead, the following assumption is made: in any r-z plane the electron heat flow is parallel to the electron flow velocity

$$\left(\vec{Q}_e \times \vec{u}_e\right)_\theta = 0$$

or

$$Q_{e,r} = Q_{e,z} \frac{u_{e,r}}{u_{e,z}} \tag{35}$$

Then from equations (8a) and (35), it follows that

$$Q_{e,r}^{(0)} = 0 \tag{36a}$$

$$Q_{e,r}^{(1)} = \frac{u_{e,r}^{(1)}}{u_{e,z}^{(0)}} Q_{e,z}^{(0)} \tag{36b}$$

The effective electron Hall parameter. - To complete the evaluation of the necessary collision integral and heat flow coefficients only requires the determination of the collision frequency $\nu_{ei}^{(0)}$. In preliminary calculations, it was found that use of the classical expression for $\nu_{ei}^{(0)}$ (see eq. (3.94) of ref. 7) gave results which were in serious disagreement with experimental data. As a result of this the classical expression for $\nu_{ei}^{(0)}$ was replaced by an effective value. In particular, the following assumption was made: the electron Hall parameter can be approximated by an effective value which is constant, at least near the axis of symmetry,

$$\omega_e^{(0)}\tau_e^{(0)} = \frac{\omega_e^{(0)}}{\nu_{ei}^{(0)}} \approxeq \text{constant} \tag{37}$$

where

$$\omega_e^{(0)} = \frac{qB(r = 0, z)}{m_e} = \frac{qB_z^{(0)}}{m_e} \tag{38}$$

This assumption is based on an analysis by Solbes (ref. 8) which predicts (using quasi-linear plane-wave analysis) that a saturation in the effective Hall parameter can result from electrothermal instabilities. In reference 8, Solbes also compares his analysis with MHD generator experimental data and obtains good agreement. The assumption (37) also permitted an analytic asymptotic solution (i.e., large z); no such solution could be found when the classical expression for $\nu_{ei}^{(0)}$ was used.

Final Equations

When expressions (32a) and (36b) are used, the momentum collision integral coefficients (eqs. (30a) to (30c)) become, respectively,

$$I_{e,z}^{(0)} = -\frac{5}{2}\frac{\gamma}{\mathcal{E}} N_e^{(0)} \frac{dkT_e^{(0)}}{dz} \tag{39a}$$

$$I_{e,r}^{(0)} = 0 \tag{39b}$$

$$I_{e,r}^{(1)} = -\frac{5}{2}\frac{\gamma}{\mathcal{E}} N_e^{(0)} \frac{dkT_e^{(0)}}{dz} \frac{u_{e,r}^{(1)}}{u_{e,z}^{(0)}} \tag{39c}$$

Then, when equations (5), (6), (8b), (8d), (C21), (31b), (32a), (36b), (37), and (39a) to (39c) are used, equations (21), (23), (25), and (28) become, respectively,

$$m_i\left\{\frac{1}{2N^2}\left[\frac{d}{dz}(Nu)\right]^2 - u\frac{d}{dz}\left[\frac{1}{N}\frac{d}{dz}(Nu)\right]\right\} + q\frac{dE}{dz} = -\frac{5}{2}\frac{\gamma}{\mathcal{E}}\frac{dkT_e}{dz}\left(\frac{d\ln u}{dz} + \frac{d\ln N}{dz}\right) \tag{40}$$

$$\frac{d}{dz}(NkT_e) + qNE = -\frac{5}{2}\frac{\gamma}{\mathcal{E}}\frac{Nd(kT_e)}{dz} \tag{41}$$

$$m_i Nu\frac{du}{dz} + \frac{d}{dz}(NkT_e) = 0 \tag{42}$$

$$\frac{3}{2}u\frac{d(kT_e)}{dz} - ukT_e\frac{d\ln N}{dz} + \frac{5}{2}\frac{(\omega_e\tau_e)}{\mathcal{E}q}\left[\frac{kT_e}{B}\frac{d(kT_e)}{dz}\frac{d\ln u}{dz} - \frac{d}{dz}\left(\frac{kT_e}{B}\frac{dkT_e}{dz}\right)\right]$$

$$+\frac{3qB}{m_i}\frac{kT_e}{(\omega_e\tau_e)} = 0 \tag{43}$$

where

$$N = N_e^{(0)} = N_i^{(0)} \tag{44a}$$

$$u = u_{e,z}^{(0)} = u_{i,z}^{(0)} \tag{44b}$$

$$T_e = T_e^{(0)} \tag{44c}$$

$$E = E_z^{(0)} \tag{44d}$$

$$B = B(r = 0, z) \tag{44e}$$

$$\omega_e = \frac{qB}{m_e} \tag{44f}$$

$$\tau_e = \tau_e^{(0)} = \frac{1}{\nu_{ei}^{(0)}} \tag{44g}$$

Equations (40) to (43) constitute four independent equations in the four unknowns N, u, T_e, and E; the effective electron Hall parameter $\omega_e\tau_e$ and the applied on-axis magnetic field (which is approximately equal to B) are assumed to be specified. The electric field E and its derivative dE/dz can be eliminated by combining equations (40)

and (41). The number density N, which occurs throughout the equations in the form d(ln N)/dz, can be eliminated by using equation (42). The final equations for the electron temperature on the axis T_e and the ion flow velocity on the axis u are then

$$\left(\frac{m_i u^2}{kT_e} - \frac{5}{2}\frac{\gamma}{\mathcal{E}}\right)\frac{d^2(kT_e)}{dz^2} - \left(\frac{m_i u^2}{2kT_e} + \frac{5}{2}\frac{\gamma}{\mathcal{E}}\right)\frac{1}{kT_e}\left(\frac{dkT_e}{dz}\right)^2$$

$$+\frac{5}{2}\frac{\gamma}{\mathcal{E}}\left(1 - \frac{m_i u^2}{kT_e}\right)\frac{d \ln u}{dz}\frac{d(kT_e)}{dz} + \frac{m_i^2 u^3}{kT_e}\frac{d^2 u}{dz^2}$$

$$+ m_i\left[\frac{3}{2} + \frac{m_i u^2}{kT_e}\left(1 + \frac{m_i u^2}{2kT_e}\right)\right]\left(\frac{du}{dz}\right)^2 = 0 \tag{45}$$

$$u\frac{d \ln(kT_e)}{dz} + \frac{2}{5}\frac{m_i u^2}{kT_e}\frac{du}{dz} + \frac{(\omega_e \tau_e)}{\mathcal{E} qB}\left[\left(\frac{d \ln u}{dz} + \frac{d \ln B}{dz} - \frac{d \ln kT_e}{dz}\right)\frac{d(kT_e)}{dz}\right.$$

$$\left. - \frac{d^2(kT_e)}{dz^2}\right] + \frac{6}{5}\frac{qB}{m_i(\omega_e \tau_e)} = 0 \tag{46}$$

For both convenience and a reduction in the numerical calculations, equations (45) and (46) can be put into dimensionless form. It is convenient to nondimensionalize the ion velocity by the final exhaust velocity, the electron thermal energy by the final ion directed energy, and the distance by the radius a of the magnetic field coils (fig. 1). Thus letting

$$x = \frac{z}{a} \tag{47a}$$

$$U = \frac{u(z)}{u(z = \infty)} = \frac{u}{u_\infty} \tag{47b}$$

$$\tau = \frac{\left(\frac{3}{2}kT_e\right)}{\left(\frac{1}{2}m_i u_\infty^2\right)} \tag{47c}$$

$$C = \frac{5}{3}\frac{\gamma}{\mathcal{E}} \tag{47d}$$

$$C_1 = \frac{3\mathcal{E}qa}{(m_i u_\infty \omega_e \tau_e)} \tag{47e}$$

equations (45) and (46) take, respectively, the following dimensionless forms:

$$U'' = \left(\frac{\tau}{6U^3}\right)\left\{\left(C + \frac{U^2}{\tau}\right)\frac{(\tau')^2}{\tau} + \left(C - \frac{2U^2}{\tau}\right)\tau'' + C\left(\frac{3U^2}{\tau} - 1\right)\frac{U'\tau'}{U}\right.$$

$$\left. - 2(U')^2\left[\frac{3}{2} + \left(\frac{3U^2}{\tau}\right)\left(1 + \frac{3}{2}\frac{U^2}{\tau}\right)\right]\right\} \tag{48}$$

$$\tau'' = \frac{2C_1^2}{5\mathcal{E}}B^2 + C_1 B\left(\frac{U\tau'}{\tau} + \frac{6}{5}\frac{U^2U'}{\tau}\right) + \tau'\left(\frac{U'}{U} + \frac{B'}{B} - \frac{\tau'}{\tau}\right) \tag{49}$$

where all derivatives are with respect to the dimensionless distance x (e.g., $\tau'' = (d^2\tau/dx^2)$). Using assumption (7) and expressions (B2) and (B3) for the applied on-axis magnetic field, equation (49) becomes

$$\tau'' = \frac{45}{2\mathcal{E}}\beta^2F^2 + \frac{15}{2}\beta F\left(\frac{U\tau'}{\tau} + \frac{6}{5}\frac{U^2U'}{\tau}\right) + \tau'\left(\frac{U'}{U} + \frac{F'}{F} - \frac{\tau'}{\tau}\right) \tag{50}$$

where

$$\beta = \frac{\sqrt{5}}{8}\frac{\mathcal{E}}{(\omega_e\tau_e)}\left(\frac{qB_{max}}{m_i}\frac{a}{u_\infty}\right) \tag{51a}$$

is a dimensionless magnetic field, and

$$F = \left(1 + x^2\right)^{-3/2} + \left[1 + (1 + x)^2\right]^{-3/2} \tag{51b}$$

$$F' = -3\left\{x\left(1 + x^2\right)^{-5/2} + (1 + x)\left[1 + (1 + x)^2\right]^{-5/2}\right\} \tag{51c}$$

In expression (51a) B_{max} is the maximum value of the applied magnetic field, occurring on the axis of symmetry midway between the two field coils (fig. 1).

Equations (48), (50), and (51) thus comprise the dimensionless set of nonlinear equations to be solved.

NUMERICAL SOLUTIONS

To the authors' knowledge equations (48), (50), and (51) do not admit analytic solutions. However, it is possible to obtain asymptotic analytic solutions for large x by expanding τ and U in power series in the variable x^{-1}. These solutions represent relations between the starting values used for the numerical solutions. Then, instead of needing four initial values (i.e., τ, U, τ', U'), it is only necessary to specify two initial values in order to begin the numerical solution at some point far downstream.

In addition to deriving the asymptotic analytic solution in this section, the numerical procedure is also discussed. Included in this discussion is the way in which experimental data were used to estimate representative values of the various parameters in the problem. This eliminated the potentially difficult problem of hunting numerically for values of these parameters that would lead to meaningful solutions.

Asymptotic Analytic Solutions

The analytic solutions for large x are based on the following series expansions:

$$\tau = \frac{A_1}{x} + \frac{A_2}{x^2} + \frac{A_3}{x^3} + \cdots \tag{52a}$$

$$U = 1 + \frac{B_1}{x} + \frac{B_2}{x^2} + \cdots \tag{52b}$$

$$N = \frac{D_1}{x} + \frac{D_2}{x^2} + \frac{D_3}{x^3} + \cdots \tag{52c}$$

There are no zero order terms in expansions (52a) and (52c) since T_e (and hence τ) and N are assumed to vanish as x approaches infinity. The zero order term in (52b) is obvious since $U(=u/u_\infty)$ approaches unity as x approaches infinity. In general, the

n^{th} term of a series such as equation (52a) could be assumed to be of the form $A_n x^{-n-\gamma_2}$; however, in appendix E it is shown that here γ_2 must be zero.

Substituting expressions (52a) and (52b) into equation (48) and equating the sum of the lowest order terms in x^{-1} to zero yield

$$A_1^2 + 4B_1A_1 + 3B_1^2 = 0 \tag{53}$$

for which there are two solutions:

$$A_1 = -B_1 \tag{54a}$$

$$A_1 = -3B_1 \tag{54b}$$

Only one of these solutions is admissible. To see this, reference is made to equation (42), which in dimensionless form is

$$3NUU' + N\tau' + \tau N' = 0 \tag{55}$$

Then to lowest order in x^{-1},

$$D_1(3B_1 + 2A_1) = 0 \tag{56}$$

From the results (54a) and (54b), it follows that

$$D_1 = 0 \tag{57}$$

Equation (55) then yields to lowest order in x^{-1}

$$3D_2(B_1 + A_1) = 0 \tag{58}$$

so that

$$A_1 = -B_1 \tag{59}$$

provided that $D_2 \neq 0$. (If $D_2 = 0$, both eqs. (54a) and (54b) are incompatible with eq. (55) and no solution exists.)

Substituting expansions (52a) and (52b) into equation (50) and equating the sum of the lowest order nonvanishing terms in x^{-1} to zero gives

$$A_2 = \frac{A_1}{3}\left(B_1 - \frac{3}{2}\right) - 5\beta\left(1 + \frac{6}{5}\frac{B_1}{A_1}\right) \tag{60}$$

Substituting equation (59) into (60) yields

$$A_2 = \frac{B_1}{3}\left(\frac{3}{2} - B_1\right) + \beta \tag{61}$$

Then, from equations (59) and (61) the asymptotic solutions (52a) and (52b) become, respectively,

$$\tau = -\frac{B_1}{x} + \frac{B_1}{3x^2}\left(\frac{3}{2} - B_1\right) + \frac{\beta}{x^2} \tag{62a}$$

$$U = 1 + \frac{B_1}{x} \tag{62b}$$

The higher order coefficients (A_3, B_2, etc.) could be determined in a similar manner in terms of B_1 and β; however, the algebra quickly becomes prohibitive. Moreover, it is anticipated that the truncated series (62a) and (62b) will be adequate for the purpose of starting the numerical solution.

From equations (62a) and (62b), the first derivatives are, in truncated form,

$$\tau' = -2\frac{\tau}{x} - \frac{B_1}{x^2} \tag{62c}$$

$$U' = -\frac{B_1}{x^2} \tag{62d}$$

These results assume, of course, that the asymptotic series (52a) and (52b) can be differentiated term by term.

Numerical Procedure

Assuming that equations (62a) to (62d) are sufficiently accurate expressions for large x, the numerical solution can be started provided the coefficient B_1 is known (β is treated as a parameter). For a given β and an arbitrary value of B_1, equations (48) and (50) are solved numerically using equations (62a) to (62d) as starting values and working upstream (i.e., decreasing values of x). The quantities obtained are x_M, the value of x for which the Mach number of the flow is unity, and

$$1/\tau_{max} = \frac{\left(\frac{1}{2} m_i u_\infty^2\right)}{\left(\frac{3}{2} k T_{e,max}\right)} \tag{63}$$

For each value of the parameter β two curves are obtained, one with x_M as a function of B_1 and one with $1/\tau_{max}$ as a function of B_1. From these sets of curves, two families of curves are obtained showing (1) the dependence of $1/\tau_{max}$ on x_M for fixed values of β, and (2) the dependence of $1/\tau_{max}$ on β for fixed values of x_M. Finally, by repeating the latter set of calculations, but with the electron energy collision integral included, it is possible to determine an upper limit on β beyond which the analysis is no longer self-consistent.

As indicated previously, the quantity $1/\tau_{max}$ (eq. (63)) is the primary goal of this analysis since it gives the ratio of the final (downstream) ion directed kinetic energy to the maximum (upstream) electron thermal energy.

Starting calculations. - In order to begin the numerical solution some estimate of the magnitude of B_1 for a given β is needed. Such an estimate can be obtained from the measurements of reference 5. In that reference,

$$a = 3.6\times10^{-2} \text{ meter} \tag{64a}$$

$$B_{max} = 2.5\times10^{-2} \text{ Tesla} \tag{64b}$$

$$m_i = 6.68\times10^{-26} \text{ kg} \tag{64c}$$

The final ion flow velocity, u_∞, of reference 5 can be calculated from the z-component of the ion momentum equation which is simply equation (42) minus equation (41):

$$\frac{m_i}{2}\frac{d(u^2)}{dz} = -q\frac{dV}{dz} + \frac{5}{2}\frac{\gamma}{\mathcal{E}}\frac{d(kT_e)}{dz} \tag{65}$$

where V is taken as the on-axis plasma potential of reference 5 (i.e., $E = E_z^{(0)} = -dV/dz$). Integrating equation (65) gives

$$\frac{m_i}{2q}\left(u_\infty^2 - u^2\right) = (V - V_\infty) - \frac{5}{2}\frac{\gamma}{\mathcal{E}}\frac{kT_e}{q} \tag{66}$$

At the calorimeter survey plane of reference 5, the following measurements were made:

$$z = 0.14 \text{ meter} \tag{67a}$$

$$\frac{m_i u^2}{2q} = 72 \text{ volts} \tag{67b}$$

$$\frac{kT_e}{q} = 5.2 \text{ volts} \tag{67c}$$

$$V = 26 \text{ volts} \tag{67d}$$

The operation of substituting equations (67b) to (67d) into equation (66) and taking $\gamma = 0.6$, $\mathcal{E} = 1.86$ (these values are those for a fully ionized gas as given in appendix D) yields

$$\frac{m_i u_\infty^2}{2q} = 94 \text{ volts} \tag{68}$$

where it has been assumed that $V_\infty = 0$ inasmuch as the plasma potential of reference 5 is measured relative to the surrounding tank walls of the experiment. If the ions were completely collision-free, the result (68) would be replaced by the simple sum of (67b) and (67d), or 98 volts; the last term on the right hand side of equation (66), which arises from the electron momentum collision integral, accounts for the difference.

From the result (eq. (68)),

$$u_\infty = 2.12\times10^4 \text{ m/sec} \tag{69}$$

Then from equations (62b), (64a), (67a), (67b), and (68), a rough estimate of B_1 is

$$B_1 \cong -0.485 \tag{70}$$

It should be emphasized that (70) is only an estimate inasmuch as there is no assurance apriori that the calorimeter survey plane of reference 5 is sufficiently far downstream to justify the use of the truncated series (eq. (62b)). This estimate is adequate, however, since all that is required here is some rough idea of where to begin the aforementioned numerical solution scheme, that is, what reasonable value of B_1 is needed for a given β value.

The appropriate value of β is found by substituting equations (64a) to (64c) and (69) into expression (51a),

$$\beta = \frac{5.3\times10^{-2}}{(\omega_e \tau_e)} \tag{71}$$

Substituting equations (64a), (67a), (70), and (71) into equation (62a) gives

$$\tau = 0.104 + \frac{3.52\times10^{-3}}{(\omega_e \tau_e)}$$

so that from equation (68),

$$\frac{kT_e}{q} = \frac{2}{3}\left(\frac{m_i u_\infty^2}{2q}\right)\tau = 6.5 + \frac{0.22}{(\omega_e \tau_e)} \tag{72}$$

For $\omega_e \tau_e \geq 1$, the result (eq. (72)) gives the following range for the electron temperature at the calorimeter survey plane:

$$6.5 \text{ volts} \leq \frac{kT_e}{q} \leq 6.72 \text{ volts} \tag{73}$$

This range differs from the measured result (eq. (67c)) by at most 30 percent. Part of this difference is undoubtedly due to the fact that the calorimeter survey plane of reference 5 is not sufficiently far downstream to justify the use of either of the truncated series (eqs. (62a) and (62b)). Nevertheless, the result (eq. (73)) is sufficiently accurate to permit the use of equations (70) and (71) as a "starting" point for the numerical solution scheme previously outlined.

As various values of B_1 and β are used some idea of the starting value of x is required. In order that the asymptotic starting solutions (eqs. (62a) to (62d)) be reasonably accurate it is necessary that the starting value $x = x_o$ be large enough to make the lowest order terms dominant. To accomplish this the following constraints are imposed on equations (62a) and (62b):

$$\frac{-B_1}{x_o} \leq 0.05$$

that is,

$$x_o \geq -20B_1 = w_1 \tag{74a}$$

$$\frac{-B_1\left(\frac{3}{2} - B_1\right)}{3x_o^2} \frac{1}{\left(-\frac{B_1}{x_o}\right)} \leq 0.05$$

that is,

$$x_o \geq \frac{20}{3}\left(\frac{3}{2} - B_1\right) = w_2 \tag{74b}$$

and

$$\frac{\frac{\beta}{x_o^2}}{\left(\frac{-B_1}{x_o}\right)} \leq 0.05$$

that is,

$$x_o \geq -20\frac{\beta}{B_1} = w_3 \tag{74c}$$

(Note that B_1 must be negative.) The requirement that the magnitude of each higher order term in equations (62a) and (62b) be less than 5 percent of the corresponding

dominant term is of course arbitrary. However, such a requirement should certainly ensure that these asymptotic starting solutions are reasonably accurate. The starting value of x is then taken to be

$$x_o = \max(w_1, w_2, w_3) \tag{74d}$$

The derivatives (eqs. (62c) and (62d)) are then automatically accurate expressions provided that the asymptotic series can be differentiated term by term.

Numerical integration. - Equations (48) and (50) were solved numerically on an IBM 7094 electronic digital computer using a fourth order Runga-Kutta technique (see, e.g., ref. 9). In order to enhance the accuracy of the results, a variable step size, Δx, was used. For the m^{th} computation the step size was

$$(\Delta x)_m = \frac{0.002(\Delta x)_{m-1}}{U_{m-2} - U_{m-1}} \tag{75}$$

with an initial step size of $(\Delta x)_0 = -0.01$. The constraint (eq. (75)), which tends to maintain ΔU at approximately 0.2 percent of the final value of U, namely unity, is again arbitrary. It should, however, certainly keep the truncation error of the Runga-Kutta scheme at a reasonably small value while also reducing the computer run time. The constraint (eq. (75)) also allows a level of accuracy not possible with a fixed step size near the upstream singularity point ($U \to 0$), where U begins to change very rapidly.

As already mentioned, one of the quantities to be calculated is x_M, the value of x where the Mach number of the flow is unity. For this purpose the Mach number must be computed at each step of the numerical solution. For simplicity, the Mach number of the flow is based on the adiabatic sound speed of the gas which is given by

$$a_s = \left(\frac{5P}{3\rho}\right)^{1/2} \tag{76}$$

where P and ρ are, respectively, the scalar pressure and mass density (on the axis) of the gas. Taking into account the fact that $m_i >> m_e$ and $T_e >> T_i$, expression (76) becomes

$$a_s \approx \left(\frac{5kT_e}{3m_i}\right)^{1/2}$$

so that the Mach number of the flow on the axis of symmetry is

$$M = \frac{u}{a_s} = \left(\frac{3m_i}{5kT_e}\right)^{1/2} u$$

which in terms of U and τ is

$$M = \frac{3U}{(5\tau)^{1/2}} \tag{77}$$

The approximate value of x_M is found by a linear interpolation in the computer program.

RESULTS AND DISCUSSION

Singularity at Maximum Electron Temperature

The results of a typical computer run are shown in figures 2 and 3. Here $\beta = 0.1$ and the sonic point is located at $x_M = 1.09$ (the coordinate $x = z/a$ is measured from the center plane of the downstream coil of fig. 1). At the point where the dimensionless electron temperature τ reached a maximum value there was an overflow in the computer storage and the computation was automatically stopped. Such an overflow occurred on every run and indicates a singularity point in equations (48) and (50). It will be recalled that the electron heat flow on the axis is, from expressions (32a) and (32b),

$$Q_{e,z}^{(0)} = -\frac{5}{2}\frac{P_e^{(0)}}{\mathcal{E} m_e \nu_{ei}^{(0)}}\frac{dkT_e^{(0)}}{dz} \tag{78}$$

Now the computer results show that the singularity point ($z = z_1$) is the point at which T_e attains its maximum value; that is, τ' goes through zero at $x = x_1$. Hence,

$$\frac{dT_e}{dz} > 0 \qquad \text{for } z < z_1$$

$$\frac{dT_e}{dz} = 0 \qquad \text{for } z = z_1$$

$$\frac{dT_e}{dz} < 0 \qquad \text{for } z > z_1$$

so that from expression (78)

$$Q^{(0)}_{e,z} < 0 \qquad \text{for } z < z_1 \tag{79a}$$

$$Q^{(0)}_{e,z} = 0 \qquad \text{for } z = z_1 \tag{79b}$$

$$Q^{(0)}_{e,z} > 0 \qquad \text{for } z > z_1 \tag{79c}$$

The results (eqs. (79a) to (79c)) imply that there is a point heat flow source located at $z = z_1$, the existence of which results in the singularity. (The assumption of zero on-axis current density rules out the possibility of any distributed heat flow source.) The accompanying computer overflow results from the fact that the singularity forces the term du/dz to become indefinitely large as z approaches z_1 from the downstream side. The details of the singularity are presented in appendix F.

The fact that the numerical solution cannot be carried through the singularity point is not catastrophic since $T_{e,max}$ occurs at the singularity. Hence, $1/\tau_{max}$, which is the quantity of interest, can indeed be calculated.

Axial Variation of Plasma Quantities

Figure 4 shows profiles of the normalized ion flow velocity U, the electron number density N/N_{max} (calculated from eq. (55)), the applied magnetic field B_{ext}/B_{max}, and the dimensionless electron temperature τ and plasma potential ΔV calculated from the dimensionless form of equation (66):

$$\Delta V \equiv \frac{V - V_\infty}{\left(\frac{m_i u_\infty^2}{2q}\right)} = 1 + \frac{5\gamma}{3\mathcal{E}}\tau - U^2 \tag{80}$$

At the point where the electron temperature reaches a maximum (just upstream of the sonic point) the ion flow velocity is rapidly increasing, while the electron number density and plasma potential are falling off sharply. The figure also shows that there is still significant ion acceleration relatively far downstream (e.g., at three coil radii downstream of the front coil, the ion flow velocity has attained less than 85 percent of its final value).

Spatial Dependence of U and τ on β

Figures 5 and 6 show the behavior of the spatial variation of U and τ as the dimensionless magnetic field β is varied over two orders of magnitude, with the sonic point fixed at $x_M \cong 0$. (This point corresponds to the center plane of the downstream coil of fig. 1). It can be seen from these figures that the on-axis ion flow velocity and electron temperature approach their final values over a shorter distance as the parameter β is decreased. Figure 6 shows that τ increases with β.

Ratio of Final Ion to Initial Electron Energy

Figure 7 shows the ratio of the final ion to initial electron energy $1/\tau_{max}$ and the sonic point location x_M plotted against the parameter B_1 for a given value of the nondimensional magnetic field β. By combining a set of such curves the final numerical results shown in figures 8 and 9(a) are obtained. Figure 8 shows the variation of the ratio of final ion to initial electron energy $1/\tau_{max}$ as a function of sonic point location for various values of β. Figure 9(a) shows this energy ratio as a function of β for various sonic point locations.

Figure 8 illustrates that $1/\tau_{max}$ is a strong function of sonic point location if the sonic point lies between 0.75 and one coil radius downstream of the center plane of the downstream coil. Figures 8 and 9(a) both show that $1/\tau_{max}$ is a strong function of β for β between 10^{-3} and 10^{-1} and sonic point locations less than one coil radius. The fact that $1/\tau_{max}$ is a decreasing function of β for a given sonic point location does <u>not</u> imply that $1/\tau_{max}$ is a decreasing function of B_{max} (see eq. (51a)). This is because the "constant" effective value of the electron Hall parameter $\omega_e\tau_e$ may well

depend on B_{max}. (The parameter $\omega_e\tau_e$ is "constant" only in the sense that, for a given system, $d(\omega_e\tau_e)/dx \cong 0$ for all x.)

The curves of figure 9(a) all approach a limiting value of $1/\tau_{max} \cong 1.66$ as β becomes large. This asymptote is simply the adiabatic solution of appendix G, that is, no electron heat flow and no electron energy loss term. The asymptote serves as a check on the accuracy of the numerical results; it also indicates the marked dependence of the results on the electron heat flow.

Limitations of Analysis

Figure 9(b) contains a set of curves similar to those shown in figure 9(a). However, in the calculation of the curves for figure 9(b) the electron energy collision integral I_E has been included (this corresponds to including the first term on the right hand side of equation (50), which is of order β^2). A comparison of figures 9(a) and (b) shows that the two sets of results are in close agreement for small values of β, with a maximum difference of about 25 percent at $\beta = 0.2$. Beyond this point, however, the two sets of results begin to differ sharply; at $\beta = 1$ no solutions exist for $x_M \lessapprox 0.7$ in the calculations which include I_E, while solutions exist for the full range of x_M up to about $\beta = 10$ in the calculations which omit I_E.

From these results it is apparent that the electron energy collision integral I_E becomes an important factor for $\beta \gtrapprox 0.2$. Now I_E represents the random kinetic energy lost by the electrons to the ions (note that I_E is negative, eq. (31b)); this transfer of energy causes the ion temperature to rise. Then, since the energy loss term becomes important for $\beta \gtrapprox 0.2$, it follows that the ion temperature must also become appreciable at this point. However, the ion temperature has been completely ignored in this analysis and in particular it has been omitted from the electron energy collision integral itself (see eqs. (31a) and (31b)). Clearly then, the analysis is inconsistent for $\beta \gtrapprox 0.2$. (The inclusion of I_E along with the simultaneous omission of T_i results in a violation of the conservation of energy.) This fact, along with rough estimates of typical values of β for low and high-power magnetoplasmadynamic arcs (e.g., eq. (71)), suggests that the analysis herein is applicable to the former but not for the latter case. The ion temperature is expected to be important for the high-power arc.

There is also a limit on the analysis for very small values of β which results from the implicit assumption that electron cyclotron radii are small compared to a characteristic length of the system (e.g., the magnetic field coil radius a). This requirement is necessary in order for the electrons to cyclotron within the device. The limit can be illustrated by noting that from equations (51a) and (63)

$$\beta \left(\frac{1}{\tau_{max}}\right)^{1/2} = \sqrt{\frac{5}{6\pi}} \frac{\mathcal{E}}{2} \left(\frac{m_e}{m_i}\right)^{1/2} \frac{1}{(\omega_e \tau_e)} \frac{a}{r_{ce}} \tag{81}$$

where a characteristic electron cyclotron radius has been defined:

$$r_{ce} = \frac{\left(\frac{8}{\pi} \frac{kT_{e,max}}{m_e}\right)^{1/2}}{\left(\frac{qB_{max}}{m_e}\right)} \tag{82}$$

The numerator of expression (82) is simply the average speed for a Maxwellian velocity distribution with temperature $T_{e,max}$ (ref. 10), while the denominator is the electron cyclotron frequency at B_{max}. (Although $T_{e,max}$ usually does not occur at B_{max}, eq. (82) nevertheless yields a typical value of the electron cyclotron radius.) If the ratio of the characteristic electron cyclotron radius to the coil radius is to be small, $r_{ce}/a \ll 1$, then from equation (81),

$$\beta \gg \sqrt{\frac{5}{6\pi}} \frac{\mathcal{E}}{2} \left(\frac{m_e}{m_i}\right)^{1/2} \frac{\frac{1}{(\omega_e \tau_e)}}{\left(\frac{1}{\tau_{max}}\right)^{1/2}} \tag{83}$$

From figure 8 the largest possible value of $1/\tau_{max}$ is less than 32, so that expression (83) becomes

$$\beta \gg 8.5 \times 10^{-2} \frac{\left(\frac{m_e}{m_i}\right)^{1/2}}{(\omega_e \tau_e)} \tag{84}$$

The inequality (84) gives an indication of the lower bound on the dimensionless magnetic field β. For the case in reference 5 (argon propellant), the requirement (84) becomes

$$\beta \gg \frac{3 \times 10^{-4}}{(\omega_e \tau_e)} \tag{85}$$

which is certainly satisfied by the experiment (see eq. (71)).

Significance of Results

The inclusion of thermal conduction in the expansion of a plasma in a magnetic nozzle yields a dramatic effect. As shown in figures 8 and 9(a), the ratio of final ion to initial electron energy can be increased more than an order of magnitude over its adiabatic expansion value.

The results of this analysis should permit one to predict the final exhaust velocity and spatial variations of the plasma quantities of a low power MPD arc thruster as a function of upstream electron temperature. However, to do so requires that one know both the location of the sonic point in the flow x_M and the value of the dimensionless magnetic field β. Although reasonable estimates of x_M and β can be made for a given device, there is at present no precise method of calculating these quantities. Thus, to compare the analysis herein with experiments requires very detailed diagnostics of the experimental plasma exhaust. The only experiment of this type is that by Bowditch (ref. 5). Unfortunately, Bowditch was unable to obtain data in the neighborhood of the sonic point because the probes were destroyed by the large heat transfer in that region. Hence, presently, no quantitative comparison can be made between the analysis herein and experiment. There does appear, however, to be qualitative agreement. Using Bowditch's data to begin the numerical solution resulted in rapid convergence of the calculations; furthermore, the asymptotic analytic solution for electron temperature (eq. (73)) agreed relatively well with Bowditch's measured value. Thus, the analysis at least appears to be consistent with available data.

One important application of the results of this analysis has been indicated. The analysis leads to specifying the maximum range of the ratio of final ion to initial electron energy. Seikel et al. (ref. 6), indicate how this information can be used in a power balance for a low power dc MPD arc to set an upper bound on both the possible efficiency as a function of specific impulse and the maximum specific impulse attainable.

CONCLUDING REMARKS

The axisymmetric expansion of a thermally conductive plasma in a magnetic nozzle has been analyzed. As an important step in the determination of an upper bound on the potential performance of applicable MPD arc thrusters, the on-axis ratio of the directed exhaust energy to the maximum (upstream) thermal energy was calculated as a function of two parameters: (1) the location of the on-axis sonic point, and (2) a dimensionless

magnetic field β, which involves the ratio of the maximum value of the applied magnetic field to an effective electron Hall parameter. The results indicate that thermal conduction can be the dominant process in the expansion inasmuch as the energy ratio can be significantly higher than that of an adiabatic expansion. The analysis appears to be valid for the low power MPD arc; the point where it becomes inconsistent indicates that the analysis must be extended by including the ion temperature to cover the case of the high power MPD arc (large β). The implicit assumption of small electron cyclotron radii sets a lower bound on β.

Lewis Research Center,
National Aeronautics and Space Administration,
Cleveland, Ohio, September 16, 1970,
120-26.

APPENDIX A

SYMBOLS

A_m	m^{th} coefficient in series for dimensionless electron temperature
a	effective radius of magnetic field coil, m
a_s	adiabatic sound speed of gas, m/sec
$\vec{B}$	magnetic flux density, T
B_m	m^{th} coefficient in series for normalized ion flow velocity
C	dimensionless force law parameter defined by eq. (47d)
C_1	parameter defined by eq. (47e), T^{-2}
$\vec{c}_e$	random electron velocity, m/sec
D_m	m^{th} coefficient in series for number density, m^{-3}
$\vec{E}$	electric field intensity, V/m
F	dimensionless function defined by eq. (51b)
I_E	electron energy collision integral, N/m^2-sec
$\vec{I}_e$	electron momentum collision integral, N/m^3
$\vec{J}$	conduction current density, A/m^2
K	constant defined by eq. (16)
k	Boltzmann constant, 1.3805×10^{-23} J/K
ℓ	length defined by fig. 10, m
M	Mach number of flow
m_e	electron rest mass, 9.109×10^{-31} kg
m_i	ion rest mass, kg
N	number density, m^{-3}
0	"of the order of"
P	scalar pressure, N/m^2
$\vec{Q}$	heat flow, J/m^2-sec
q	electron charge, 1.602×10^{-19} C
r	radial coordinate, m
$\hat{r}$	unit vector in r-direction
T	temperature, K
t	time, sec
U	normalized ion flow velocity
u	flow velocity, m/sec
u_∞	final ion flow velocity, m/sec
V	plasma potential, V
$\vec{v}$	total particle velocity, m/sec
w_1, w_2, w_3	defined by eq. (74)
x	dimensionless axial distance
z	axial coordinate, m
z'	dimensionless force law parameter

β	dimensionless magnetic field defined by eq. (51a)
γ	dimensionless force law parameter
Δx	step size for numerical analysis
ϵ	diffusion Mach number
ϵ_o	permittivity of free space, F/m
θ	azimuthal coordinate, radians
$\hat{\theta}$	unit vector in θ-direction
μ_o	permeability of free space, H/m
ν_{ei}	effective electron-ion momentum transfer collison frequency, sec^{-1}
ξ	dimensionless force law parameter
ρ	mass density, kg/m^{-3}
τ	dimensionless electron temperature
τ_e	$1/\nu_{ei}$
ω_e	electron cyclotron frequency, rad/sec

Subscripts:

e	electron
ext	applied field
i	ion
ind	induced field
M	x_M is value of x where Mach number is unity
m	step number in numerical analysis
max	maximum value
r	radial component
z	axial component
o	starting value for numerical solution
θ	azimuthal component

Superscripts:

(m)	m^{th}-order term with respect to r
*	z* is plane where ions are created

APPENDIX B

THE APPLIED MAGNETIC FIELD

A typical magnetic field coil configuration of MPD arcs is shown in figure 10. It is assumed here that the two field coils are closely wrapped and sufficiently narrow so that the magnetic flux density near the axis can be accurately determined on the basis of two equivalent single turn loops. Each such loop carries a current equal to the current in the actual coil multiplied by the number of turns of the actual coil, and has a radius (the dimension a of fig. 10) such that the magnetic flux density of the two loops is approximately equal to that of the actual coils, at least near the centerline.

For simplicity, it is assumed that $a = \ell$ in figure 10, as is the actual case in reference 5. The magnetic flux density on the centerline due to the external coils, B_{ext}, is then (see ref. 11)

$$B_{ext}(r = 0, z) = \frac{5\sqrt{5}}{16} B_{max} \left\{ \left(1 + \frac{z^2}{a^2} \right)^{-3/2} + \left[1 + \left(1 + \frac{z}{a} \right)^2 \right]^{-3/2} \right\} \quad \text{(B1)}$$

where B_{max} is the maximum value of the applied magnetic field on the axis, occurring midway between the coils, at $z = -(\ell/2) = -(a/2)$. Substituting $x = z/a$ into expression (B1) yields

$$B_{ext}(x) = \frac{5\sqrt{5}}{16} B_{max} \left\{ \left(1 + x^2 \right)^{-3/2} + \left[1 + (1 + x)^2 \right]^{-3/2} \right\} \quad \text{(B2)}$$

and then

$$\frac{dB_{ext}(x)}{dx} = \frac{5\sqrt{5}}{16} B_{max} \left\{ -3x \left(1 + x^2 \right)^{-5/2} - 3(1 + x) \left[1 + (1 + x)^2 \right]^{-5/2} \right\} \quad \text{(B3)}$$

The analytic asymptotic solution of equation (50) requires the evaluation of the expressions in braces in equations (B2) and (B3) for large x. The binomial expansions of

$$F(x) = \left(1 + x^2 \right)^{-3/2} + \left[1 + (1 + x)^2 \right]^{-3/2} \quad \text{(B4)}$$

and

$$\frac{dF(x)}{dx} = -3x\left(1+x^2\right)^{-5/2} - 3(1+x)\left[1+(1+x)^2\right]^{-5/2} \tag{B5}$$

are, respectively,

$$F(x) = 2x^{-3} - 3x^{-4} + 3x^{-5} - \frac{5}{2}x^{-6} + 0\,(x^{-7}) \tag{B6}$$

and

$$\frac{dF(x)}{dx} = -6x^{-4} + 12x^{-5} - 15x^{-6} + 0\,(x^{-7}) \tag{B7}$$

Finally, from the symmetry of the configuration shown in figure 10 it is obvious that

$$B_{\theta,\,ext} \equiv 0 \tag{B8}$$

APPENDIX C

MAGNITUDE OF FIELD QUANTITIES

Magnetic Field

The induced magnetic field is governed by the equation

$$\nabla \times \vec{B}_{ind} = \mu_o \vec{J} \tag{C1}$$

the z-component of which

$$\frac{1}{r}\frac{\partial}{\partial r}(rB_{\theta,ind}) = \mu_o J_z \tag{C2}$$

since $\partial/\partial\theta \equiv 0$. Integrating equation (C2) with respect to r yields

$$B_{\theta,ind} = \left(\frac{\mu_o}{r}\right)\int rJ_z(z,r)dr + \frac{h(z)}{r} \tag{C3}$$

The arbitrary function h(z) in expression (C3) must vanish identically in order that $B_{\theta,ind}$ be finite at $r = 0$. Hence, since $J_z = 0(r)$, assumption (6), it follows that

$$B_{\theta,ind} = 0(r^2) \tag{C4}$$

The θ-component of the total magnetic field is then

$$B_\theta = B_{\theta,ind} = 0(r^2) \tag{C5}$$

since $B_{\theta,ext} = 0$ by symmetry (see appendix B).

The divergence of the total magnetic field is

$$\nabla \cdot \vec{B} = 0 \tag{C6}$$

from which

$$\frac{1}{r}\frac{\partial}{\partial r}(rB_r) + \frac{\partial B_z}{dz} = 0 \tag{C7}$$

since $\partial/\partial\theta \equiv 0$. Integrating equation (C7) with respect to r yields

$$B_r = -\left(\frac{1}{r}\right)\int r\,\frac{\partial B_z(r,z)}{\partial z}\,dr + \frac{g(z)}{r} \tag{C8}$$

where the arbitrary function g(z) must be identically zero in order that B_r be finite on the axis. Hence, to first order in r,

$$B_r = -\left(\frac{r}{2}\right)\frac{dB_z(0,z)}{dz} \tag{C9}$$

so that

$$B_r^{(0)} = 0 \tag{C10}$$

and

$$B_r^{(1)} = -\frac{1}{2}\frac{dB(0,z)}{dz} \tag{C11}$$

Electric Field

Because of the assumption of steady-state conditions the curl of the total electric field is given by

$$\nabla \times \vec{E} = 0 \tag{C12}$$

Hence, $\vec{E}$ can be expressed in terms of the gradient of some scalar function

$$\vec{E} = -\nabla\Phi \tag{C13}$$

the θ-component of which

$$E_\theta = -\frac{1}{r}\frac{\partial}{\partial\theta} \tag{C14}$$

Then since $\partial/\partial\theta \equiv 0$,

$$E_\theta \equiv 0 \tag{C15}$$

The divergence of the total electric field is

$$\nabla \cdot \vec{E} = \left(\frac{q}{\epsilon_o}\right)(N_i - N_e) \tag{C16}$$

from which

$$\frac{1}{r}\frac{\partial}{\partial r}(rE_r) + \frac{\partial E_z}{\partial z} = \left(\frac{q}{\epsilon_o}\right)(N_i - N_e) \tag{C17}$$

since $\partial/\partial\theta \equiv 0$. Integrating equation (C17) with respect to r, and recognizing that E_r must be finite at $r = 0$, yields

$$E_r = -\left(\frac{1}{r}\right)\int r\,\frac{\partial E_z(r,z)}{\partial z}\,dr + \left(\frac{q}{\epsilon_o r}\right)\int r(N_i - N_e)dr \tag{C18}$$

Hence, to first order in r,

$$E_r = -\left(\frac{r}{2}\right)\frac{dE_z(0,z)}{dz} \tag{C19}$$

since $N_i^{(0)} = N_e^{(0)}$, assumption (5). Then

$$E_r^{(0)} = 0 \tag{C20}$$

and

$$E_r^{(1)} = -\frac{1}{2}\frac{dE_z^{(0)}}{dz} \tag{C21}$$

Conduction Current Density

With the assumption of steady-state conditions the conservation of charge equation becomes

$$\nabla \cdot \vec{J} = 0 \tag{C22}$$

from which

$$\frac{1}{r}\frac{\partial}{\partial r}(rJ_r) + \frac{\partial J_z}{\partial z} = 0 \tag{C23}$$

since $\partial/\partial\theta \equiv 0$. Substituting the r-expansions for J_r and J_z into equation (C23), and using the assumption $J_z^{(0)} = 0$, yields

$$J_r^{(0)} = J_r^{(1)} = 0 \tag{C24}$$

APPENDIX D

THE ELECTRON HEAT FLOW

The material in this appendix is based on reference 7. Equation (5.4) of that reference is the equation for the species' heat flow in a general gas system. For the case of electron heat flow in a fully ionized gas, the equation becomes

$$\frac{-\omega_e}{B}\left(\vec{B}\times\vec{Q}_e\right) + \frac{5}{2}\frac{kP_e}{m_e}\nabla T_e = \delta\left(\frac{1}{2}m_e c_e^2\vec{c}_e\right) - \frac{5}{2}\frac{kT_e}{m_e}\delta\left(m_e\vec{c}_e\right) \tag{D1}$$

where $\vec{c}_e = \vec{v} - \vec{u}_e$, with $\vec{v}$ being the total particle velocity, and where $\delta\left[(1/2)m_e c_e^2\vec{c}_e\right]$ and $\delta(m_e\vec{c}_e)$ are, respectively, the total electron heat flow collision integral and the total electron momentum collision integral for elastic collisions (the δ-notation is that used in ref. 7). In equation (D1) the traceless pressure term has been ignored, in accordance with assumption (3). Equation (D1) is based on the "transport approximation" to the Boltzmann equation. This approximation is applicable to plasmas which satisfy two conditions: (1) the species' distribution functions are close to their Maxwellian forms, and (2) the small non-Maxwellian parts are slowly varying functions of the time and spatial coordinates in the sense that their characteristic times and lengths are much larger than the corresponding collision times or mean free path lengths. Condition (1) has already been assumed in the calculation of the collision integral coefficients in the text. Insofar as equation (D1) is concerned, and in view of assumptions (1) and (3), condition (2) can be replaced by the requirement that the characteristic length for the variation of the electron heat flow, $\vec{Q}_e$, be large compared to the electron mean free path length.

The derivation of the collision integrals in equation (D1) is extremely tedious and only the results will be given here. To first order in the diffusion Mach number, ϵ, and in the dimensionless heat flows $\dfrac{Q_e}{P_e(2kT_e/m_e)^{1/2}}$ and $\dfrac{Q_i}{P_i(2kT_i/m_i)^{1/2}}$, the electron momentum collision integral is (eq. (3.42) of ref. 7),

$$\delta(m_e\vec{c}_e) = m_e N_e \nu_{ei}\left[(\vec{u}_i - \vec{u}_e) + \frac{\gamma\vec{Q}_\epsilon}{P_e}\right] \tag{D2}$$

where the assumption $Q_i/m_i \ll Q_e/m_e$ has been used. To the same level of accuracy the electron-electron heat flow collision integral is (eq. (3.50) of ref. 7)

$$\delta\left(\frac{1}{2} m_e c_e^2 \vec{c}_e\right)_{ee} = - \left(\frac{2\sqrt{2}}{5}\right) \nu_{ei} \vec{Q}_e \tag{D3}$$

where a term involving the "Coulomb logarithm" has been omitted, with the condition that $\ln \Lambda_{ei} >> 1/2$. Typical values of $\ln \Lambda_{ei}$, which depends on T_e and N_e, are about 10 (see ref. 12). The electron-ion heat flow collision integral is (eq. (3.45) of ref. 7)

$$\delta\left(\frac{1}{2} m_e c_e^2 \vec{c}_e\right)_{ei} = \left(\frac{\nu_{ei}}{2}\right)\left[5(1 - \gamma) P_e \left(\vec{u}_i - \vec{u}_e\right) + (7z' - 5\gamma - 2)\vec{Q}_e\right] \tag{D4}$$

where z' is a dimensionless number which is dependent on the interparticle force law (the γ used here is the z of ref. 7). The total electron heat flow collision integral is given by the sum of equations (D3) and (D4). Then from equations (D2) to (D4) the right-hand side of equation (D1) is

$$\vec{I} = - \left(\frac{\nu_{ei}}{2}\right)\left[5\gamma P_e \left(\vec{u}_i - \vec{u}_e\right) + 2\mathcal{E}\vec{Q}_e\right] \tag{D5}$$

where

$$\mathcal{E} = 5\gamma + 1 + \frac{2\sqrt{2}}{5} - \frac{7}{2} z' \tag{D6}$$

The z-component of equation (D1) is, to zero order in r,

$$\frac{5}{2} \frac{k P_e^{(0)}}{m_e} \frac{dT_e^{(0)}}{dz} = I_z^{(0)} = - \mathcal{E} \nu_{ei}^{(0)} Q_{e,z}^{(0)} \tag{D7}$$

where equations (C5), (C10), and (6) have been used. Hence, from equation (D7),

$$Q_{e,z}^{(0)} = - \frac{5}{2} \frac{P_e^{(0)}}{\mathcal{E} m_e \nu_{ei}^{(0)}} \frac{dkT_e^{(0)}}{dz} \tag{D8}$$

The θ-component of equation (D1) yields

$$Q_{e,r} = -\frac{B}{\omega_e B_z} I_\theta + \frac{B_r}{B_z} Q_{e,z} \tag{D9}$$

since $\partial/\partial\theta \equiv 0$, while the r-component yields

$$Q_{e,\theta} = \frac{B}{\omega_e B_z}\left(I_r - \frac{5}{2}\frac{P_e}{m_e}\frac{\partial kT_e}{\partial r}\right) + \frac{B_\theta}{B_z} Q_{e,z} \tag{D10}$$

Substituting equation (D10) into (D5) gives

$$I_\theta = -\left(\frac{\nu_{ei}}{2}\right)\left[5\gamma P_e\left(\vec{u}_i - \vec{u}_e\right)_\theta + \frac{2\mathcal{E}B}{\omega_e B_z}\left(I_r - \frac{5}{2}\frac{P_e}{m_e}\frac{\partial kT_e}{\partial r}\right) + \frac{2\mathcal{E}B_\theta}{B_z} Q_{e,z}\right] \tag{D11}$$

Substituting I_r from equation (D5) into (D11) gives

$$\begin{aligned} I_\theta = \left(\mathcal{E}\nu_{ei}\right)^2 \frac{B}{\omega_e B_z} Q_{e,r} - \left(\frac{\nu_{ei}}{2}\right)\Bigg[& 5\gamma P_e\left(\vec{u}_i - \vec{u}_e\right)_\theta \\ & - 5\mathcal{E}\gamma \frac{B}{B_z}\frac{\nu_{ei}}{\omega_e} P_e\left(\vec{u}_i - \vec{u}_e\right)_r \\ & - 5\mathcal{E}\frac{B}{B_z}\frac{P_e}{m_e\omega_e}\frac{\partial kT_e}{\partial r} + 2\mathcal{E}\frac{B_\theta}{B_z} Q_{e,z}\Bigg] \end{aligned} \tag{D12}$$

Finally, substituting equation (D12) into (D9) yields

$$\begin{aligned} Q_{e,r} = \left(\frac{\omega_e\tau_e}{2}\right)\left(\frac{B}{B_z}\right)\left[(\omega_e\tau_e)^2 + \mathcal{E}^2\frac{B^2}{B_z^2}\right]^{-1} \Bigg\{ & -5\mathcal{E}\frac{P_e}{m_e\omega_e}\frac{B}{B_z}\frac{\partial kT_e}{\partial r} \\ & + 5\gamma P_e\left[\left(\vec{u}_i - \vec{u}_e\right)_\theta - \frac{\mathcal{E}}{\omega_e\tau_e}\frac{B}{B_z}\left(\vec{u}_i - \vec{u}_e\right)_r\right] + 2\left(\mathcal{E}\frac{B_\theta}{B_z} + \frac{B_r}{B}\omega_e\tau_e\right) Q_{e,z}\Bigg\} \end{aligned} \tag{D13}$$

Now, $u_{e,\theta}^{(0)} = 0$ in order for the limit $\lim_{r\to 0} u_{e,\theta}\,\hat{\theta}$ to exist; similarly, $T_e^{(1)} = 0$ in order

no loss of generality is incurred by using the asymptotic expansion (eq. (52b)). Similarly, let

$$\tau = x^{-\gamma_2} \sum_{j=0}^{\infty} A_j x^{-j} \tag{E7}$$

$$N = x^{-\gamma_3} \sum_{j=0}^{\infty} D_j x^{-j} \tag{E8}$$

where

$$\gamma_2 \geq 0, \; A_o \neq 0 \tag{E9}$$

$$\gamma_3 > 0, \; D_o \neq 0 \tag{E10}$$

Note from expression (E10) that γ_3 is taken to be positive since $N \to 0$ as $x \to \infty$, which is obvious from physical considerations. The result $\tau \to 0$ as $x \to \infty$, which is not as obvious, can be shown by reference to equation (55):

$$3NUU' + N\tau' + \tau N' = 0 \tag{E11}$$

If τ does contain a zero order term, then clearly $\gamma_2 = 0$. Then substituting equations (E6) to (E8) into (E11) yields, to lowest order in x^{-1},

$$(\text{terms of order } x^{-m}) - \gamma_3 A_o D_o x^{-\gamma_3 - 1} = 0 \tag{E12}$$

where

$$m \geq \gamma_3 + 2 \tag{E13}$$

Clearly, since the last term in equation (E12) is the dominant one, at least one of the factors γ_3, A_o, D_o must vanish, but this is not possible in view of equations (E9) and (E10). Hence, a contradiction has been reached and it follows that τ cannot contain a zero order term. The expansion (E7) then becomes

$$\tau = x^{-\gamma_2} \sum_{j=0}^{\infty} A_j x^{-j} \tag{E14}$$

where now

$$\gamma_2 > 0, \; A_o \neq 0 \tag{E15}$$

To determine γ_2, the expansions (E6) and (E14) are substituted into equation (48) which yields, to lowest order in x^{-1},

$$\gamma_2(\gamma_2 + 2)A_o^2 x^{-2\gamma_2-2} + 6n(n+1)A_o B_n x^{-\gamma_2-n-2} + 9n^2 B_n^2 x^{-2n-2} = 0$$

$$B_n \neq 0, \; n \geq 1 \tag{E16}$$

where it has been assumed that B_n is the first nonzero coefficient beyond B_o in the expansion for U. If $\gamma_2 < n$, then clearly the first term in equation (E16) is the lowest order term, which requires

$$\gamma_2(\gamma_2 + 2)A_o^2 = 0$$

which is not possible in view of the conditions in equation (E15). Next, if $\gamma_2 > n$, then the last term in equation (E16) is the lowest order term, which requires

$$B_n = 0$$

but this case must also be ruled out since B_n was stipulated to be nonzero. The remaining case is $\gamma_2 = n$ which makes all the terms in equation (E16) of the same order, and yields

$$(n+2)A_0^2 + 6(n+1)A_o B_n + 9nB_n^2 = 0 \tag{E17}$$

The two solutions of equation (E17) are

$$A_o = -\left(\frac{3n}{n+2}\right)B_n, \; -3B_n \tag{E18}$$

It is not possible to explicitly determine the value of n inasmuch as equations (50) and (55) provide no information in this regard. However, by comparing the calculated values of kT_e/q with the measured values of reference 5, the "choice" $B_1 \neq 0$ can be shown to be the best one. Assuming the first solution in equation (E18) and considering only the lowest order x-dependent terms, the expansions (E6) and (E14) become, respectively,

$$U \cong 1 + B_n x^{-n}$$

$$\tau \cong A_o x^{-n} = - \left(\frac{3n}{n+2}\right) B_n x^{-n}$$

so that

$$\tau \cong \left(\frac{3n}{n+2}\right)(1 - U)$$

and

$$\frac{kT_e}{q} \cong \frac{2}{3}\left(\frac{m_i u_\infty^2}{2q}\right)\left(\frac{3n}{n+2}\right)(1 - U) \qquad \text{(E19)}$$

Substituting equations (67b) and (68) into (E19) gives

$$\frac{kT_e}{q} \cong 23.4\left(\frac{n}{n+2}\right) \text{ volts} \qquad \text{(E20)}$$

at the survey plane of reference 5. Then, for instance,

$$\frac{kT_e}{q} \cong 7.8 \text{ volts} \qquad \text{for } n = 1$$

$$\frac{kT_e}{q} \cong 11.7 \text{ volts} \qquad \text{for } n = 2$$

Since $n/(n+2)$ is a strictly increasing function of n, it is clear that the calculated values of kT_e/q increase with increasing values of n. The measured value of kT_e/q is

$$\frac{kT_e}{q} = 5.2 \text{ volts}$$

so that clearly the choice $n = 1$ is the most suitable one. Note that the second solution in equation (E18) is not allowable since equation (E11) is, to lowest order in x^{-1} using equations (E6), (E8), and (E14),

$$D_o\left[3nB_n + (n + \gamma_3)A_o\right] = 0 \tag{E21}$$

which becomes upon substitution of the second solution in equation (E18),

$$-3B_n\gamma_3 D_o = 0$$

A contradiction has thus been reached since B_n, γ_3, and D_o are all nonzero. Hence, the expansion (E14) becomes, with $\gamma_2 = n = 1$,

$$\tau = \sum_{j=0}^{\infty} A_j x^{-1-j}, \quad A_o = -B_1 \neq 0 \tag{E22}$$

which has the same form as the series assumed in equation (52a).

Finally, substituting the first solution in equation (E18) into (E21) gives

$$\gamma_3 = 2 \tag{E23}$$

Note that the result (eq. (E23)) is independent of both n and B_n. Hence, the expansion (E8) becomes

$$N = \sum_{j=0}^{\infty} D_j x^{-2-j}, \quad D_o \neq 0 \tag{E24}$$

which is identical in form to the series (eq. (52c)) inasmuch as the first coefficient in that series is shown to be zero (eq. (57)).

APPENDIX F

THE SINGULARITY POINT

As mentioned in the text, the singularity point can be traced to the fact that the term du/dz becomes indefinitely large as z approaches z_1 from the downstream side (i.e., as $z \to z_1^+$), where z_1 is the coordinate where the electron temperature attains its maximum value. To see this, reference is made to equations (50) and (55). Noting that

$$\lim_{x \to x_1^+} \tau' = 0 \text{ (through negative values)} \tag{F1}$$

and

$$\lim_{x \to x_1^+} \tau'' < 0 \tag{F2}$$

equation (50) becomes, in the limit as $x \to x_1^+$,

$$\tau''(x_1) = \frac{45}{2\mathcal{E}} \beta^2 F^2(x_1) + \frac{9\beta F(x_1)}{\tau_{max}} \lim_{x \to x_1^+} (U^2 U') + \lim_{x \to x_1^+} \left(\frac{\tau' U'}{U} \right) \tag{F3}$$

where it has been assumed that U remains finite as $x \to x_1^+$. Now, if $\lim_{x \to x_1^+} U' > 0$, then from expressions (F2) and (F3) it follows that

$$\lim_{x \to x_1^+} \left(\frac{\tau' U'}{U} \right) < 0 \tag{F4}$$

Then, from expressions (F1) and (F4) it follows that

$$\lim_{x \to x_1^+} \left(\frac{U'}{U} \right) = +\infty \tag{F5}$$

Hence, either

$$\lim_{x \to x_1^+} U' = +\infty \tag{F6}$$

or

$$\lim_{x \to x_1^+} U = 0 \text{ (through positive values)} \tag{F7}$$

or both (F6) and (F7) occur. However, it can be shown from equation (55) that (F7) can only occur if (F6) also occurs. Equation (55) is, in the limit as $x \to x_1^+$,

$$3 \lim_{x \to x_1^+} (UU') + \tau_{max} \lim_{x \to x_1^+} \left(\frac{N'}{N}\right) = 0 \tag{F8}$$

Hence, if $\lim_{x \to x_1^+} U = 0$, it follows that

$$\lim_{x \to x_1^+} U' = +\infty$$

since $\lim_{x \to x_1^+} N' < 0$. Hence, in any event,

$$\lim_{x \to x_1^+} U' = +\infty \tag{F9}$$

The fact that U' increases indefinitely as $x \to x_1^+$ results in an overflow in the computer storage. Several of the computed results show that U actually goes through zero and U' becomes prohibitively large as τ' approaches zero through negative values. The fact that U becomes slightly negative, in contradiction to (F7), is simply due to the inaccuracy of the Runga-Kutta scheme at the singularity point with respect to the rapidly varying function U.

APPENDIX G

THE ADIABATIC SOLUTION

In the adiabatic expansion there is no heat flow and no energy loss term. Under these conditions equation (28) becomes

$$\frac{3}{2} u \frac{dP_e}{dz} - \frac{5}{2} P_e u \frac{d \ln N}{dz} = 0 \tag{G1}$$

where $P_e = P_e^{(0)}$. Using the relation $P_e = NkT_e$, equation (G1) yields

$$\frac{3}{2} \frac{d \ln kT_e}{dz} - \frac{d \ln N}{dz} = 0 \tag{G2}$$

Equation (25), which remains unchanged,

$$m_i N u \frac{du}{dz} + \frac{dP_e}{dz} = 0 \tag{G3}$$

can be written as

$$\frac{d \ln N}{dz} = - \frac{d \ln kT_e}{dz} - \frac{m_i u}{kT_e} \frac{du}{dz} \tag{G4}$$

Combining equations (G2) and (G4) yields

$$\frac{5}{2} \frac{dkT_e}{dz} + m_i u \frac{du}{dz} = 0 \tag{G5}$$

which in nondimensional form is

$$\tau' + \frac{6}{5} UU' = 0 \tag{G6}$$

The solution of equation (G6) is simply

$$\tau + \frac{3}{5} U^2 = \text{constant} = \tau_{max} + \frac{3}{5} U_1^2 \tag{G7}$$

where U_1 is the value of U at the point x_1 where τ reaches its maximum value. Now, as $x \to \infty$, $\tau \to 0$ and $U \to 1$, so that from equation (G7),

$$\frac{1}{\tau_{max}} = \frac{5}{3} \frac{1}{\left(1 - U_1^2\right)} \tag{G8}$$

From equation (G6) it follows that

$$U_1 = U(x_1) = 0 \tag{G9}$$

or

$$U'(x_1) = 0 \tag{G10}$$

the latter implying U is a minimum at x_1, or both (G9) and (G10) occur. In any event, it is permissible to neglect U_1^2 in equation (G8), so that, finally,

$$\left(\frac{1}{\tau_{max}}\right)_{adiabatic} \approx \frac{5}{3} \tag{G11}$$

The results shown in figure 9(a) were obtained using equation (50) with the first term on the right side omitted, that is, no energy loss term,

$$\tau'' = \frac{15}{2} \beta F \frac{U}{\tau} \left(\tau' + \frac{6}{5} UU'\right) + \tau' \left(\frac{U'}{U} + \frac{F'}{F} - \frac{\tau'}{\tau}\right) \tag{G12}$$

As $\beta \to \infty$, it follows from equation (G12) that

$$\tau' + \frac{6}{5} UU' \to 0 \qquad \text{(for all } x\text{)} \tag{G13}$$

in order for the term containing β to remain finite. The consequence (eq. (G13)) is simply the adiabatic equation (G6), of course, and it follows that the asymptote of figure 9(a) is simply the adiabatic solution given by equation (G11).

REFERENCES

1. Seikel, G. R.: Generation of Thrust - Electromagnetic Thrustors. In Electric Propulsion for Spacecraft, NASA SP-22, 1962, pp. 19-24.

2. Domitz, S.: Experimental Evaluation of a Direct-Current Low-Pressure Plasma Source. NASA TN D-1659, 1963.

3. Meyerand, R. G., Jr.; Salz, F.; Lary, E. C.; and Walch, A. P.: Electrostatic Potential Gradients in a Nonthermal Plasma. In Proceedings of the Fifth Int. Conf. Ionization Phenomena in Gases, vol. 1, 1961, H. Maecker, ed., North-Holland Publ. Co., 1962, pp. 333-342.

4. Seikel, G. R.; Bowditch, D. N.; and Domitz, S.: Application of Magnetic-Expansion Plasma Thrustors to Satellite Station Keeping and Attitude Control Missions. Paper no. 64-677, AIAA, Aug. 1964.

5. Bowditch, D. N.: Investigation of the Discharge and Exhaust Beam of a Small Arc Plasma Thrustor. Paper no. 66-195, AIAA, Mar. 1966.

6. Seikel, G. R.; Connolly, D. J.; Michels, C. J.; Richley, E. A.; Smith, J. M.; and Sovie, R. J.: Plasma Physics of Electric Rockets. Proceedings of the Conference on Plasmas and Magnetic Fields in Propulsion and Power Research, NASA SP-226, 1969, pp. 1-64.

7. Walker, E. L.: Transport Phenomena of General Non-Equilibrium Gas Systems. Ph.D. Thesis, Case Institute of Technology, 1967.

8. Solbes, A.: Quasi-Linear Plane Wave Study of Electrothermal Instabilities. In Electricity from MHD, vol. I, Proceedings of a Symposium on Magnetohydrodynamic Electrical Power Generation, International Atomic Energy Agency, 1968, pp. 499-518.

9. McCracken, D. D.; and Dorn, W. S.: Numerical Methods and Fortran Programing. John Wiley & Sons, Inc., 1968, p. 325.

10. Delcroix, J. L. (Melville Clark, Jr.; David J. BenDaniel; and Judith M. BenDaniel, trans.): Introduction to the Theory of Ionized Gases. Interscience Publishers, Inc., 1964, p. 30.

11. Plonsey, R.; and Collin, R. E.: Principles and Applications of Electromagnetic Fields. McGraw-Hill Book Company, Inc., 1961, p. 208.

12. Spitzer, L.: Physics of Fully Ionized Gases. Second ed., Interscience Publishers, 1967, p. 128.

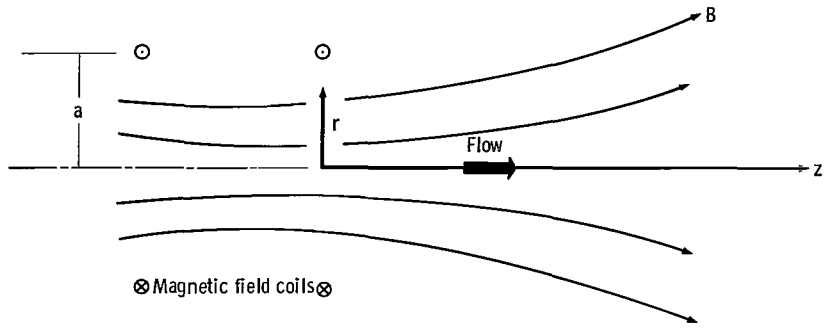

Figure 1. - Plasma expansion in a magnetic nozzle.

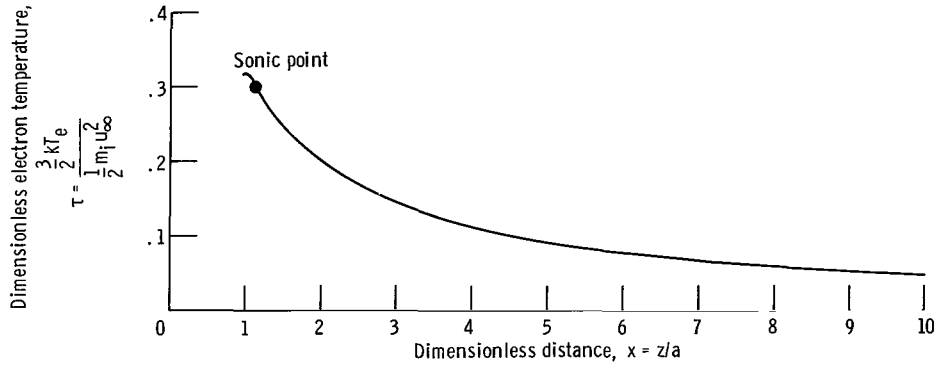

Figure 2. - Dimensionless on axis electron temperature τ as function of dimensionless distance x for dimensionless magnetic field $\beta = 10^{-1}$ and sonic point location $x_M = 1.09$.

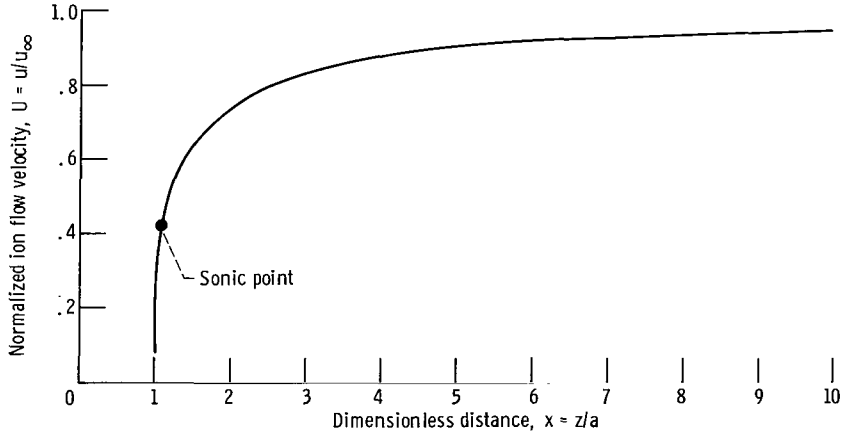

Figure 3. - Normalized on axis ion flow velocity U as function of dimensionless distance x for dimensionless magnetic field $\beta = 10^{-1}$ and sonic point location $x_M = 1.09$.

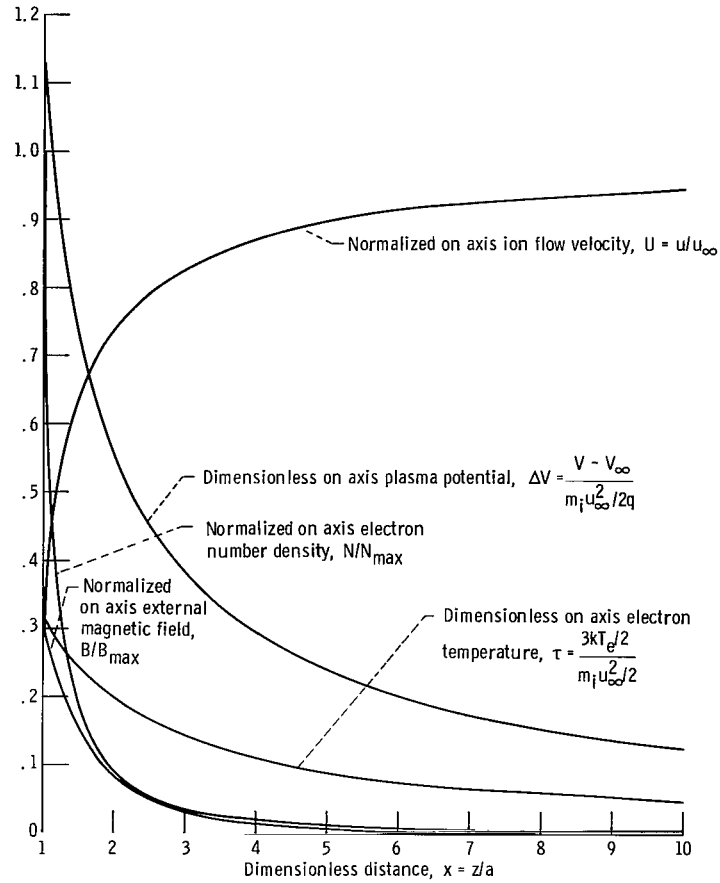

Figure 4. - Axial profiles of plasma properties for dimensionless magnetic field $\beta = 10^{-1}$ and sonic point location $x_M = 1.09$.

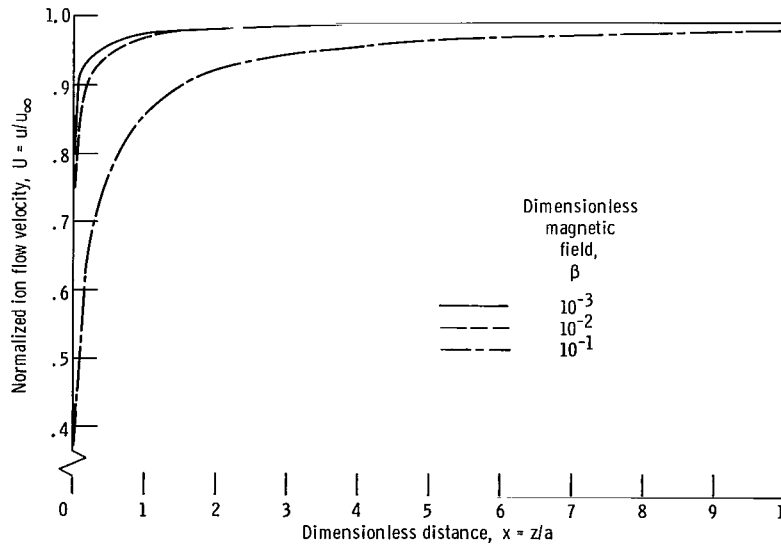

Figure 5. - Normalized on axis ion flow velocity U as function of dimensionless distance x with dimensionless magnetic field β as parameter. Sonic point location $x_M \cong 0$.

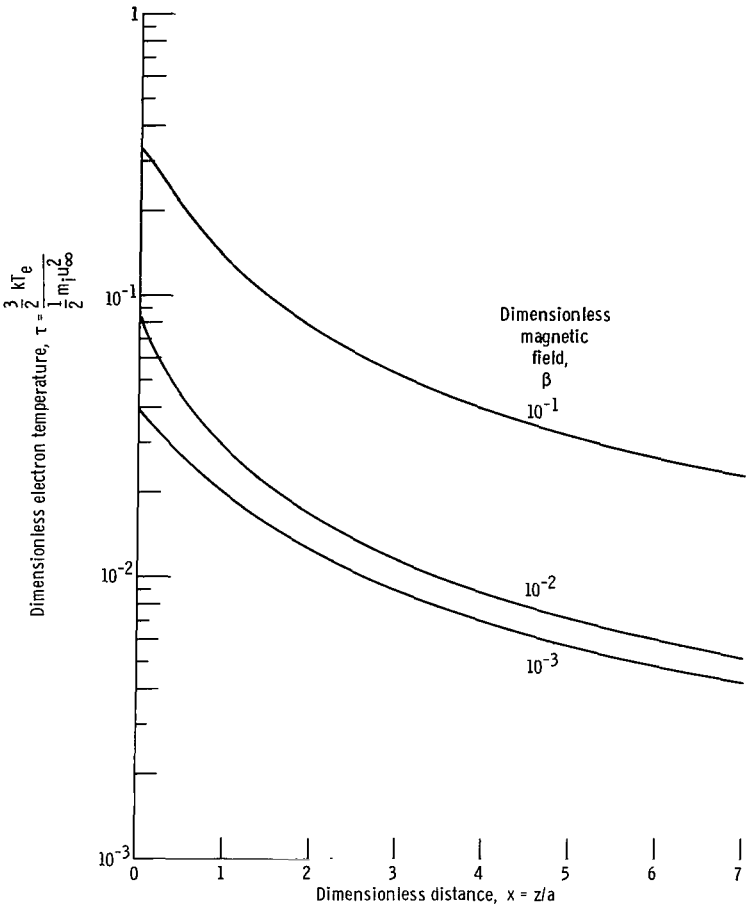

Figure 6. - Dimensionless on axis electron temperature τ as function of dimensionless distance x with dimensionless magnetic field β as parameter. Sonic point location, $x_M \cong 0$.

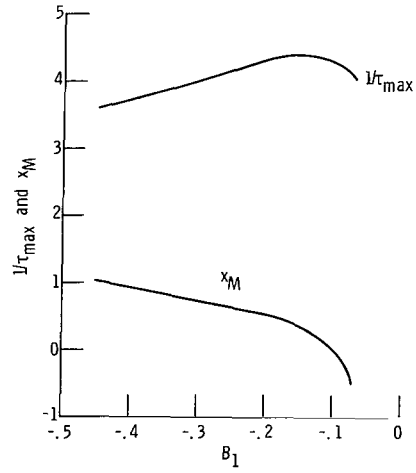

Figure 7. - Ratio of final ion to initial electron energy $1/\tau_{max}$ and sonic point location x_M as function of parameter B_1 for dimensionless magnetic field $\beta = 5 \times 10^{-2}$.

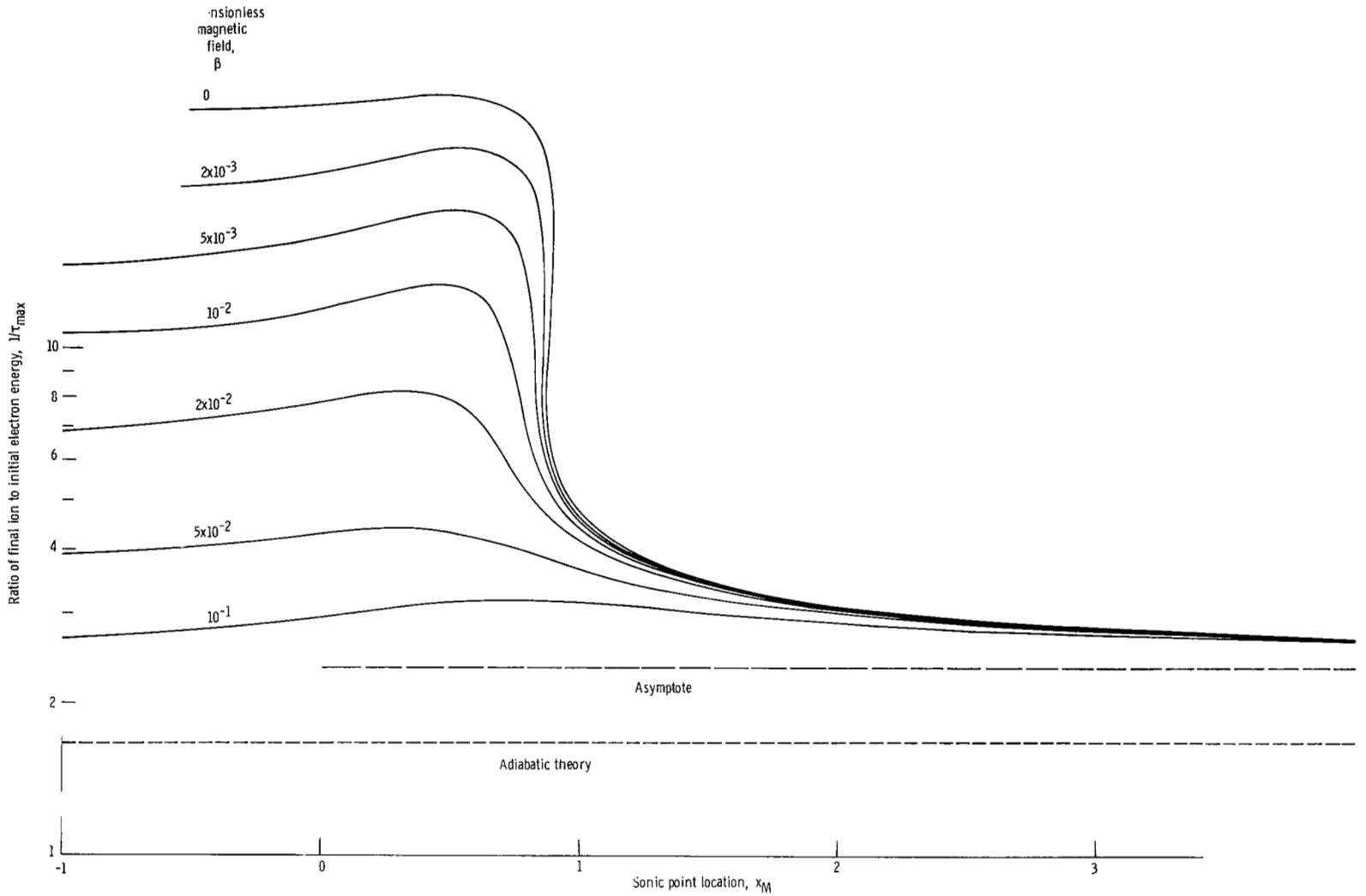

Figure 8. - Ratio of final ion to initial electron energy $1/\tau_{max}$ as function of sonic point location x_M with dimensionless magnetic field β as parameter

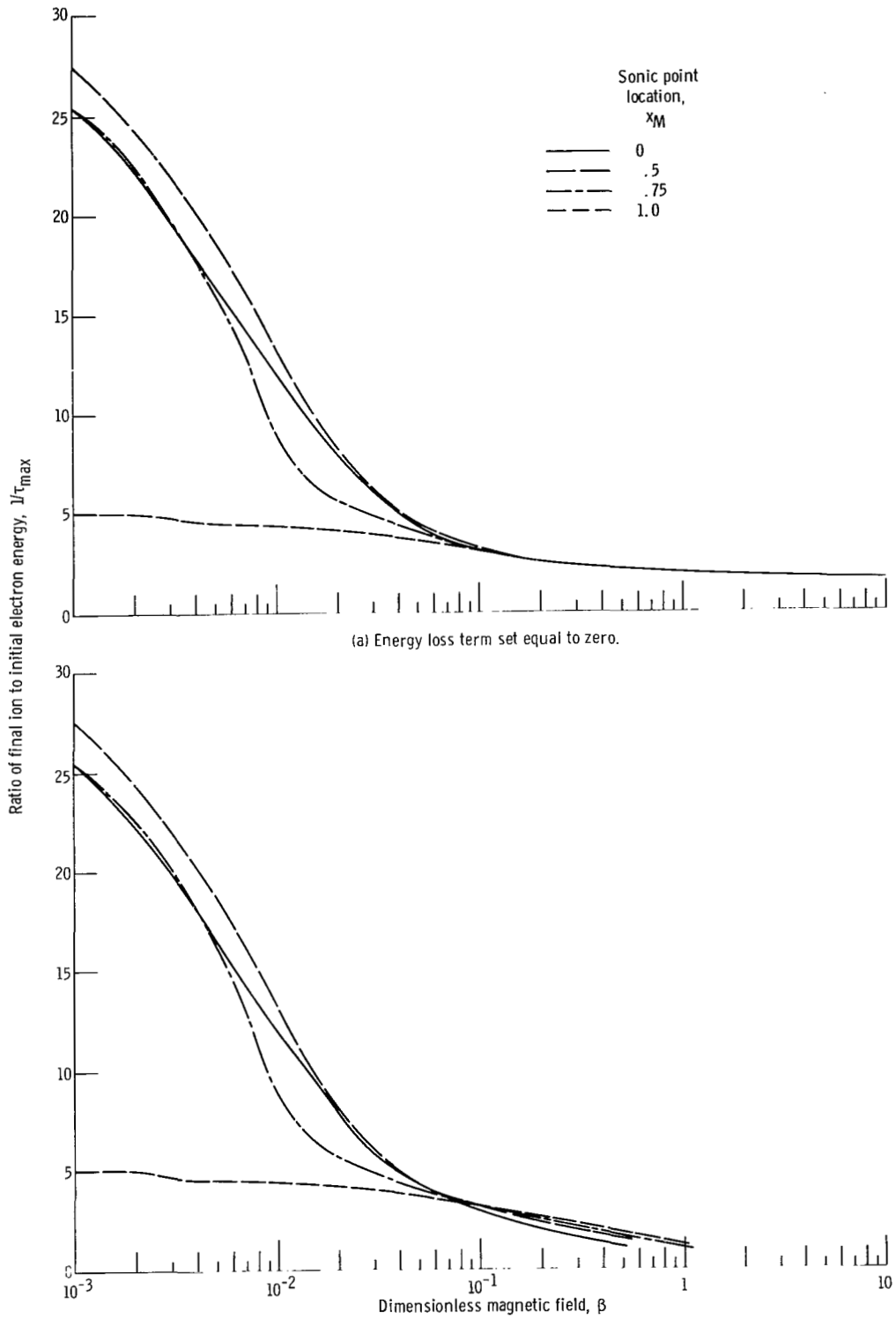

(a) Energy loss term set equal to zero.

(b) Energy loss term included.

Figure 9. - Ratio of final ion to initial electron energy $1/\tau_{max}$ as function of dimensionless magnetic field β with the sonic point location x_M as parameter.

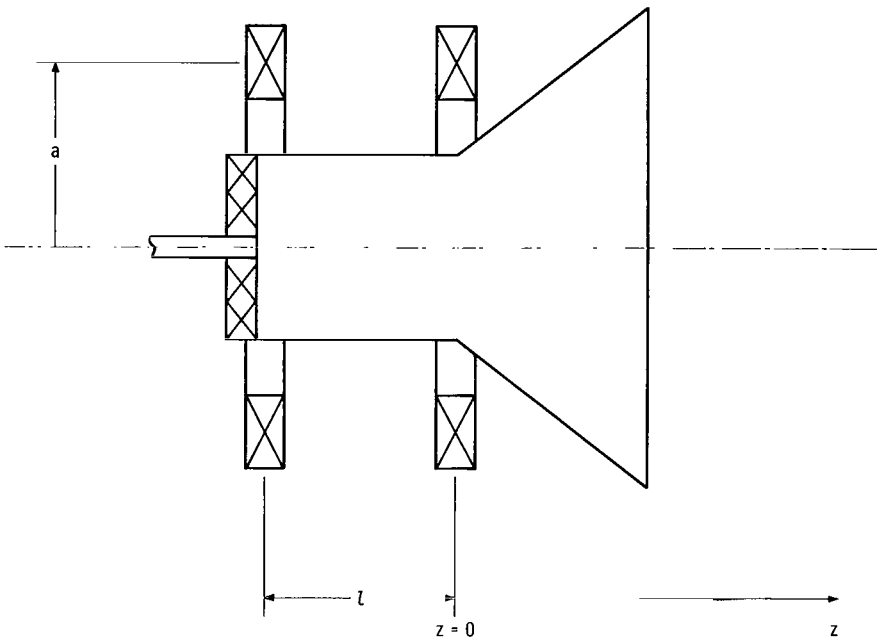

Figure 10. - Typical configuration of MPD arc thrusters.

"The aeronautical and space activities of the United States shall be conducted so as to contribute . . . to the expansion of human knowledge of phenomena in the atmosphere and space. The Administration shall provide for the widest practicable and appropriate dissemination of information concerning its activities and the results thereof."

— NATIONAL AERONAUTICS AND SPACE ACT OF 1958

NASA SCIENTIFIC AND TECHNICAL PUBLICATIONS

TECHNICAL REPORTS: Scientific and technical information considered important, complete, and a lasting contribution to existing knowledge.

TECHNICAL NOTES: Information less broad in scope but nevertheless of importance as a contribution to existing knowledge.

TECHNICAL MEMORANDUMS: Information receiving limited distribution because of preliminary data, security classification, or other reasons.

CONTRACTOR REPORTS: Scientific and technical information generated under a NASA contract or grant and considered an important contribution to existing knowledge.

TECHNICAL TRANSLATIONS: Information published in a foreign language considered to merit NASA distribution in English.

SPECIAL PUBLICATIONS: Information derived from or of value to NASA activities. Publications include conference proceedings, monographs, data compilations, handbooks, sourcebooks, and special bibliographies.

TECHNOLOGY UTILIZATION PUBLICATIONS: Information on technology used by NASA that may be of particular interest in commercial and other non-aerospace applications. Publications include Tech Briefs, Technology Utilization Reports and Technology Surveys.

Details on the availability of these publications may be obtained from:

SCIENTIFIC AND TECHNICAL INFORMATION OFFICE

NATIONAL AERONAUTICS AND SPACE ADMINISTRATION

Washington, D.C. 20546